This is an open access article published under an ACS AuthorChoice License, which permits copying and redistribution of the article or any adaptations for non-commercial purposes.

energy&fuels

Article

pubs.acs.org/EF

Diesel Surrogate Fuels for Engine Testing and Chemical-Kinetic Modeling: Compositions and Properties

Charles J. Mueller,[*,†] William J. Cannella,[‡] J. Timothy Bays,[§] Thomas J. Bruno,[∥] Kathy DeFabio,[‡] Heather D. Dettman,[⊥] Rafal M. Gieleciak,[⊥,¶] Marcia L. Huber,[∥] Chol-Bum Kweon,[#] Steven S. McConnell,[▽] William J. Pitz,[○] and Matthew A. Ratcliff[◆]

[†]Sandia National Laboratories, 7011 East Avenue, MS 9053, Livermore, California 94550, United States

[‡]Chevron Energy Technology Company, 100 Chevron Way, Richmond, California 94801, United States

[§]Pacific Northwest National Laboratory, 902 Battelle Boulevard, Richland, Washington 99352, United States

[∥]National Institute of Standards and Technology, 325 Broadway, Boulder, Colorado 80305, United States

[⊥]Natural Resources Canada (CanmetENERGY), 1 Oil Patch Drive, Devon, Alberta, Canada T9G 1A8

[#]U.S. Army Research Laboratory, 4603 Flare Loop Road, Aberdeen Proving Ground, Maryland 21005, United States

[▽]Marathon Petroleum Company, 539 South Main Street, Findlay, Ohio 45840, United States

[○]Lawrence Livermore National Laboratory, 7000 East Avenue, Livermore, California 94550, United States

[◆]National Renewable Energy Laboratory, 15013 Denver West Parkway, Golden, Colorado 80401, United States

Supporting Information

ABSTRACT: The primary objectives of this work were to formulate, blend, and characterize a set of four ultralow-sulfur diesel surrogate fuels in quantities sufficient to enable their study in single-cylinder-engine and combustion-vessel experiments. The surrogate fuels feature increasing levels of compositional accuracy (i.e., increasing exactness in matching hydrocarbon structural characteristics) relative to the single target diesel fuel upon which the surrogate fuels are based. This approach was taken to assist in determining the minimum level of surrogate-fuel compositional accuracy that is required to adequately emulate the performance characteristics of the target fuel under different combustion modes. For each of the four surrogate fuels, an approximately 30 L batch was blended, and a number of the physical and chemical properties were measured. This work documents the surrogate-fuel creation process and the results of the property measurements.

1. INTRODUCTION

Significant cost savings, efficiency gains, and emissions reductions are possible through the computational co-optimization of engines and evolving commercial fuels. A number of technological advancements are required to achieve this goal, including sufficiently accurate (1) compositional characterization of commercial fuels,[1,2] (2) models for the thermodynamic and transport properties of the compounds comprising commercial fuels,[3,4] (3) chemical-kinetic oxidation models for mixtures of compounds representative of those present in commercial fuels,[5−11] (4) computational models for the physical/thermodynamic processes occurring within the engine including interactions with the kinetics of ignition and combustion,[9,10,12−17] (5) numerical algorithms and computational hardware that can complete the required calculations in an acceptable amount of time,[15,18,19] and (6) experimental capabilities to verify the extent to which items 1−5 have been achieved.[12,20−24] The cited references provide some recent examples showing that considerable progress has been made in these areas for diesel fuel since a recent review.[5] The primary focus of this work is to further address aspects 1−3 and 6, for diesel fuel in reciprocating compression-ignition engine applications.

The composition of a typical commercial diesel fuel is too complex to model exactly,[25] so it is of interest to create a surrogate fuel, i.e., a simpler mixture that captures the essential performance characteristics of the commercial diesel fuel to sufficient accuracy, but for the sake of computational tractability contains only approximately 10 or fewer pure "palette" compounds. Because the composition of a fuel uniquely determines its properties and performance characteristics at a given engine operating condition, the approach taken in this study was to characterize the composition of the commercial "target fuel" using the best available analytical techniques, and then select and employ representative surrogate palette compounds to closely match the target-fuel compositional characteristics and key properties. Fuel properties are largely interdependent.[26] As a result, once a sufficient number of the key properties have been matched between the target and surrogate fuels, other target-fuel properties that were not explicitly selected for emulation by the surrogate should be accurately reproduced as well,[25] providing some confirmation that the surrogate formulation is sound.

Received: December 9, 2015
Published: January 7, 2016

 © 2016 American Chemical Society

DOI: 10.1021/acs.energyfuels.5b02879
Energy Fuels 2016, 30, 1445−1461

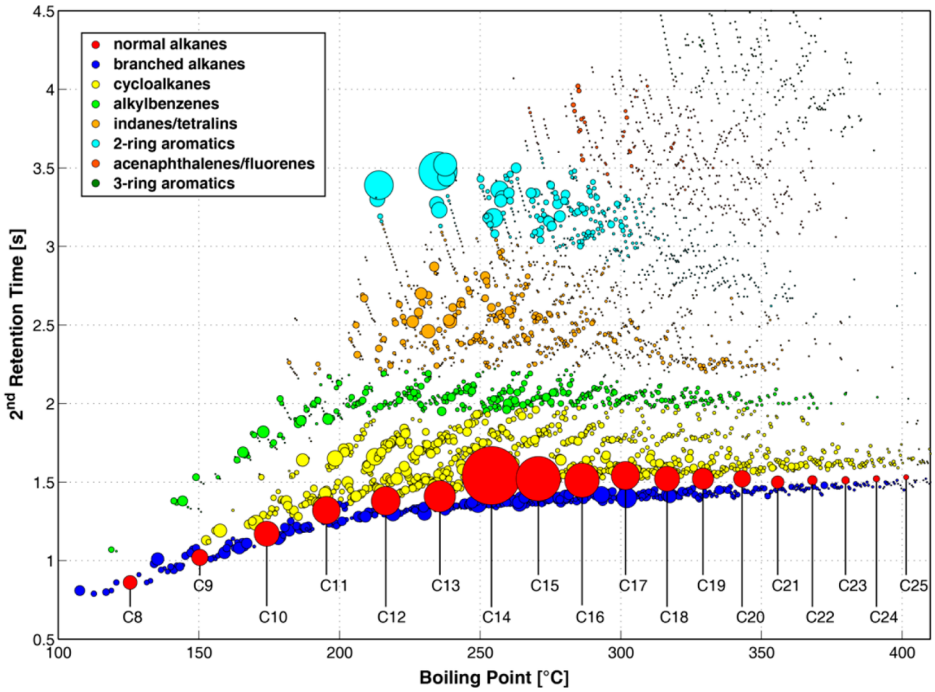

Figure 1. GC×GC-FID chromatogram for no. 2 diesel certification fuel (CF), acquired using "normal" column configuration. Annotations showing the carbon numbers and boiling points of the individual *n*-alkanes are provided for reference. The second retention time is proportional to polarity/polarizability. The three-ring aromatic content of CF is difficult to discern because it is so low.

Albert Einstein has been quoted as saying, "Everything should be made as simple as possible, but not simpler."[27] This concept certainly applies to the creation of surrogate fuels, where it is of primary importance to determine how much compositional accuracy the surrogate fuel must have in order to adequately match the performance of the target fuel.[28] Typically, the answer to this question will depend on the details of the intended application. A related question with application-specific answers is whether fuel-composition effects are large enough to justify the increased computational cost that comes with increased surrogate-fuel compositional accuracy (e.g., computational cost has been shown to scale with the cube of the number of species in a detailed chemical-kinetic mechanism[29]).

Lower-compositional-accuracy diesel surrogate fuels are usually composed of a smaller number of readily available compounds, often with lower purities. Such surrogates are frequently used because they are relatively inexpensive and easy to procure, blend, and computationally model. Some potential drawbacks of lower-compositional-accuracy surrogates are: sufficient property matching is not possible; the effects of the impurities are unknown or large; and some of their primary constituents are not representative of compounds found in commercial diesel fuels (e.g., 2,2,4,4,6,8,8-heptamethylnonane[25] and/or compounds whose molecular weights are too low). Higher-compositional-accuracy surrogates are usually composed of a larger number of palette compounds in higher purities, with molecular structures and weights that are more representative of those found in commercial diesel fuels. Such surrogates are desirable because they can provide a better match to the target-fuel composition and properties. The downsides of higher-accuracy surrogates include the higher costs associated with high-purity, ultralow-sulfur, representative palette compounds; the increased complexities of treating and blending processes; and greater difficulties in kinetic modeling.

To address these and other issues, the research described herein was conducted to create a set of chemically and physically well-characterized, high-purity, ultralow-sulfur diesel surrogate fuels that can be studied experimentally and numerically to better understand the many trade-offs between surrogate compositional accuracy on one hand and simplicity on the other. Using the eight-component "version 1" (V1) surrogate for the CFA target fuel from our previous study[25] as a baseline, two lower-accuracy surrogates and one higher-accuracy surrogate were formulated. The lower-accuracy surrogates, denoted V0a and V0b, are composed of four and five palette compounds, respectively. V0a contains palette compounds that have been used in other studies,[15,16] and V0b is similar but contains a compound to better match the heavy end of the distillation curve. The higher-accuracy, nine-component surrogate, denoted V2, provides the best match to the compositional characteristics of the target fuel and contains five new palette compounds.

This work describes the formulation, blending, and property testing of ∼30 L batches of the V0a, V0b, V1, and V2 diesel surrogate fuels to support planned future testing in compression-ignition engines, combustion vessels, and other experimental setups. The goal of the testing is to quantify the extent to which each surrogate emulates the target-fuel performance over a wide range of applications and to provide insights into the underlying reasons for any disagreements. The experimental results will also be compared to numerical simulations using the same surrogate fuels, to assist in identifying and overcoming barriers to accurate and cost-effective computational fuel/engine system optimization.

2. MATERIALS AND METHODS

This section covers target-fuel characterization techniques; palette-compound selection; the regression model used to formulate the surrogate fuels; the procurement, safe handling, analysis, treatment,

DOI: 10.1021/acs.energyfuels.5b02879
Energy Fuels 2016, 30, 1445−1461

and additization of the palette compounds; and the blending of the surrogate fuels.

2.1. Target-Fuel Characterization. The target fuel for this study was a grade no. 2-D S15 diesel[30] emissions-certification fuel from Chevron-Phillips Chemical Co.,[31] denoted in this work as CF. This is one of the same target fuels (including batch number) that was used in our previous work,[25] and Table 1 therein provides many of the properties of CF as previously measured. Table S1 in the Supporting Information shows the CF specifications as originally provided by the supplier. Although there can be wide variability in commercial diesel fuels,[32] CF was deemed to be sufficiently representative of an average commercial diesel fuel in North America to be selected as the target fuel for this research.

Because one objective of this research was to match target- and surrogate-fuel compositional characteristics as closely as possible (as opposed to matching properties alone), a hybrid approach was employed to precisely and accurately quantify the target-fuel composition. First, the composition of CF was characterized using two-dimensional gas chromatography with flame ionization detection (GC×GC-FID) techniques.[1,2] This perspective was critical for identifying and selecting palette compounds that are representative of the actual constituent molecules of the CF target fuel. Second, proton-decoupled ^{13}C (carbon-13) and ^{1}H (proton) NMR spectroscopy techniques were used to determine the mole fractions of 11 different carbon types (CTs) in CF, as shown in Figure 7 of our previous paper[25] and described therein. (The 11 CTs are also shown in Figure 3 of the current paper.) The CT mole fractions determined for CF were used in a regression model to blend the selected palette compounds such that each surrogate fuel matched these CT mole fractions as closely as possible within the other constraints of the regression model (see section 2.3).

2.1.1. Two-Dimensional Gas Chromatography with Flame Ionization Detection. A GC×GC-FID chromatogram for CF is shown in Figure 1. This chromatogram was generated using the "normal" column configuration, wherein the first column separates the constituent compounds by boiling point and the second column separates by polarity/polarizability.[1] The mass fraction of each constituent compound is proportional to the area of its corresponding colored circle in Figure 1,[2] and different hydrocarbon structural classes are indicated with different colors. Many different hydrocarbon classes are evident in Figure 1, including normal alkanes, branched alkanes, cycloalkanes, aromatics, and naphthoaromatics.

Figure S1a in the Supporting Information shows a GC×GC-FID chromatogram for CF that was generated using an alternative, "reversed" column configuration, wherein the first semipolar column separates the constituent compounds by polarity/polarizability and volatility, and the second nonpolar column separates primarily by volatility. This alternative approach enables more-accurate separation of cycloalkanes into one-ring, two-ring, and multiring subgroups, as well as improved differentiation from other hydrocarbon classes (see section 3.1.2) but otherwise gives information that is generally similar to that shown in Figure 1. Details of the GC columns and temperature programs used in the separations are provided elsewhere.[1]

The normal- and reversed-column GC×GC-FID chromatograms for the CF target fuel that are shown in Figure 1 and Supporting Information Figure S1a, respectively, were each separately measured three times. The normal GC×GC-FID chromatogram for CF was found to comprise 3723 individual peaks, with a standard deviation over the three replicates of 83 peaks, whereas the reversed-column GC×GC-FID chromatogram comprised 4969 ± 81 individual peaks. This indicates that the CF target fuel contains on the order of 5000 individual compounds/isomers, because each peak nominally corresponds to at least one compound/isomer (i.e., peaks corresponding to different species can overlap on the chromatogram). This is believed to be the first published quantification of the number of species in diesel fuel.

There was some concern that the bulk composition of the CF target fuel may have changed due to weathering and/or degradation between this group's first publication[25] and the current study. GC×GC-FID was used to address this concern by quantitatively comparing chromatograms acquired in early 2013 vs late 2014. No significant differences in bulk composition (>0.5 wt %) were observed. Nevertheless, it was found that the derived cetane number (DCN) of CF was gradually increasing over time. This might be due to peroxide formation, because peroxides can affect ignition delay even when they are only present at parts per million levels.[33] This phenomenon is discussed in more detail in section 3.2.

2.1.2. NMR Spectroscopy. The technique for using ^{13}C and ^{1}H NMR spectroscopy to classify the carbon atoms in the CF target fuel into 11 distinct types and quantitatively determine the mole fraction of each of these types is described in detail in previous research.[25,34] A key feature of this approach is the estimation of C and H mole fractions in the fuel from the CT mole fractions determined from NMR spectroscopy. When the carbon content of the NMR dataset was set to that measured by elemental analysis, the NMR-derived hydrogen content was found to be within 0.8 wt % of that measured by elemental analysis.[35]

The results of the previous analysis of CF were used in the current study, with one exception. The reversed-column GC×GC-FID results for CF, which were conducted after the previous publication[25] and are considered more accurate, showed a higher level of >1.2 wt % cycloalkanes with three or more rings. Based on the known range of structures of those cycloalkanes and the potential impacts on the sooting tendency of a fuel from cycloalkane dehydrogenation (to aromatics), the target mole fraction for CT6 (CH bridgehead between two cycloalkane rings; see Figure 3) was revised upward from 0.81 to 1.61 mol %. To compensate for this increase, the target mole fraction of CT3 (branched-alkane CH; see Figure 3) was decreased from 5.70 to 4.90 mol %, which kept the CT3 mole fraction within its uncertainty bounds. V0a, V0b, and V2 were formulated using these new target CT mole fractions, whereas the V1 formulation had been determined previously, using the original target CT mole fractions. The CT mole fractions for the target and surrogate fuels are defined and illustrated in Figure 3 (CF, V0a, and V2) and Supporting Information Figure S3 (CF, V0b, and V1).

2.2. Palette-Compound Selection. Palette-compound selection is an exercise in balancing multiple trade-offs, including the following: molecular structure, molecular weight, ignition quality, boiling point, melting point, density, viscosity, availability, purity (including isomeric), cost, safety, and availability of detailed and/or reduced chemical-kinetic oxidation mechanisms. No palette compound is perfect in all respects, though some are certainly more desirable than others. The fundamental trade-off is that the branched alkanes, cycloalkanes, aromatics, and naphthoaromatics that are truly representative of those found in commercial diesel fuels are challenging to procure in high purity and with low sulfur content, and hence few of their property data are available in the literature.

The palettes for the surrogates with lower compositional accuracy (V0a and V0b) were composed of compounds used in simpler surrogates from the literature. These simpler palettes are subsets of the palette for the V1 surrogate for CF, which is shown in Figure 9 of our previous paper.[25] For the V2 surrogate, however, four of the compounds in the V1 palette for CF were replaced with five new compounds that are more representative of species found in commercial diesel fuels, while still facilitating procurement and kinetic modeling, but at potentially higher cost. All of the palette compounds are shown in Figure 2, and selected properties are provided in Table 1, including references to detailed and/or lumped chemical-kinetic (C-K) oxidation mechanisms (a dash indicates that no mechanism could be found in the literature or online). All palette compounds contained <15 ppmw of sulfur and were supplied at ≥98 wt % purity. Table 2 provides the number of carbon atoms of each CT in each palette-compound molecule, information that is required for determining the CT mole fractions in the surrogate fuels.

The five new compounds that were added to the V2 surrogate palette were selected to improve its ability to match the composition and properties of the CF target fuel, as follows. First, *n*-eicosane (NEI) was selected to facilitate better matching of the heavy end of the distillation curve. Second, 2-methylheptadecane (2MHPD) was selected to replace HMN as the branched-alkane compound in the

DOI: 10.1021/acs.energyfuels.5b02879
Energy Fuels 2016, 30, 1445−1461

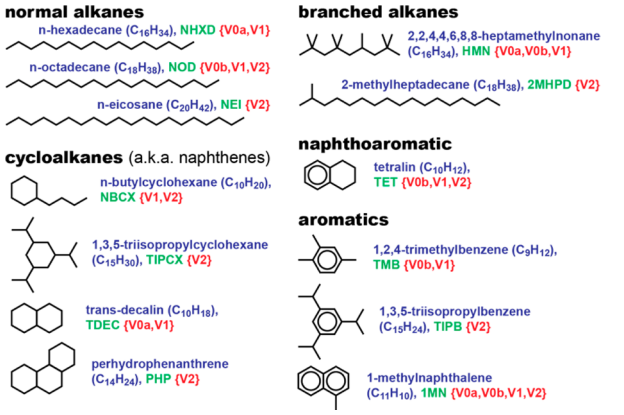

Figure 2. Surrogate palette compounds. For each palette compound, the abbreviation of the compound name is shown in green text after the chemical formula of the compound, and the red text enclosed by curly braces indicates the surrogate fuels that contain the compound.

V2 palette, because 2MHPD is more representative than HMN of the types of branched alkanes found in commercial diesel fuels, and because the starting material for 2MHPD synthesis (methyl palmitate) is relatively inexpensive. This being said, all representative diesel-range branched alkanes are relatively expensive, and 2MHPD is certainly no exception (see Table 4). Despite their high costs, it was decided to keep a branched alkane in the palette to mitigate problems with fuel solidification at low temperatures and/or high pressures (see section 3.5.3). Third, 1,3,5-triisopropylbenzene (TIPB) and 1,3,5-triisopropylcyclohexane (TIPCX) were added to the palette because they are characteristic of the multiply substituted, low-cetane, C_{14} and larger monoaromatics and monocycloalkanes, respectively, that are found in commercial diesel fuels. The structural similarity between TIPB and TIPCX (in terms of identical substituents at analogous locations around a central, six-membered ring) was compelling because it could simplify kinetic modeling and because TIPCX can be produced by hydrogenating TIPB, simplifying procurement. Some key data for TIPCX were not initially available, but these have since been measured.[24,52] Finally, perhydrophenanthrene (PHP) was selected because it reasonably represents the polycycloalkanes found in commercial diesel fuels and can be produced by hydrogenating phenanthrene, which is readily available at 98% purity for a reasonable cost.

One trade-off involved in including TIPCX and PHP in the V2 palette was that they have two[24] and five[53] isomers, respectively, that are not easily separated and may have different physical or chemical properties (as has been observed with decalin isomers[54]). The enhanced compositional accuracy afforded by including TIPCX and PHP in the V2 palette was deemed worthy of this additional complexity. The isomer fractions will not change if the production conditions for the compounds are held constant, which seems likely if the same suppliers are used.

Table 2. Number of Carbon Atoms of Each Carbon Type in Each Palette-Compound Molecule

Palette Compound Abbrev.	Carbon Type (CT) 1	2	3	4	5	6	7	8	9	10	11
NHXD	2	14	0	0	0	0	0	0	0	0	0
NOD	2	16	0	0	0	0	0	0	0	0	0
NEI	2	18	0	0	0	0	0	0	0	0	0
HMN	9	3	1	0	0	0	0	0	0	0	3
2MHPD	3	14	1	0	0	0	0	0	0	0	0
NBCX	1	3	0	5	1	0	0	0	0	0	0
TIPCX	6	0	3	3	3	0	0	0	0	0	0
TDEC	0	0	0	8	0	2	0	0	0	0	0
PHP	0	0	0	10	0	4	0	0	0	0	0
TMB	3	0	0	0	0	0	3	3	0	0	0
TIPB	6	0	3	0	0	0	3	3	0	0	0
TET	0	0	0	4	0	0	4	0	2	0	0
1MN	1	0	0	0	0	0	7	1	0	2	0

2.3. Regression Model. Although changes to the surrogate-formulation approach were considered (e.g., adding cost as a surrogate-design parameter, matching hydrocarbon-class mass fractions from GC×GC-FID rather than carbon types from NMR spectroscopy, and switching to a volatility parameter that could be measured to the end boiling point of the fuel and modeled with publicly available software), it was decided to use the same surrogate-formulation approach as in our previous work,[25] to better elucidate the effects of changing the palette compounds without the confounding effects of employing a new methodology. The design parameters were as follows: composition as quantified by mole fraction of each CT,[25] ignition quality as quantified by the derived cetane number (DCN),[55] volatility as quantified by the advanced distillation curve (ADC),[56−58] and density.[59] As in our previous work, the goal was to match the 11 CTs, DCN, ADC points, and density to within 3 mol %, 1.5 numbers, ±7 °C, and 5%, respectively, between CF and each surrogate. The same procedure was used to formulate the V0a, V0b, and V2 surrogates as was used to formulate the V1 surrogate, as described in

Table 1. Selected Properties of the Palette Compounds

palette compd name	abbrev	CAS no.	mol wt (g/mol)	MP[a] (°C)	BP[b] (°C)	density[c] (kg/m^3)	DCN[d]	LHV[e,36] (MJ/kg)	C-K mech available?
n-hexadecane	NHXD	544-76-3	226.4	17.9	286.8	756	100[g]	43.946	yes[37−42]
n-octadecane	NOD	593-45-3	254.5	27.9	316.8	766	106[43]	43.897	–
n-eicosane	NEI	112-95-8	282.5	36.9	343.8	774	110[43]	43.854	–
heptamethylnonane[f]	HMN	4390-04-9	226.4	–	246.4	768	15.1	43.853	yes[37,38,44,45]
2-methylheptadecane	2MHPD	1560-89-0	254.5	4.8	311.1	763	91	43.937	yes[39]
n-butylcyclohexane	NBCX	1678-93-9	140.3	−74.9	183.0	785	47.6	43.418	yes[46]
1,3,5-triisopropylcyclohexane	TIPCX	34387-60-5	210.4	–	~250[24]	809	23.6	43.532	–
trans-decalin	TDEC	493-02-7	138.2	−31.2	187.3	851	31.8	42.538	yes[47]
perhydrophenanthrene	PHP	5743-97-5	192.3	–	–	928	37.8	43.461	–
1,2,4-trimethylbenzene	TMB	95-63-6	120.2	−46.2	169.4	856	8.9	41.024	yes[48]
1,3,5-triisopropylbenzene	TIPB	717-74-8	204.4	−7.4	236.3	836	2.9	41.987	–
tetralin	TET	119-64-2	132.2	−35.2	207.7	949	8.9	40.525	yes[47]
1-methylnaphthalene	1MN	90-12-0	142.2	−29.2	244.8	986	0[g]	39.352	yes[49,50]

[a]Melting point at 0.10 MPa from NIST Webbook[51] unless noted otherwise. [b]Boiling point at 0.10 MPa from NIST Webbook[51] unless noted otherwise. [c]From NIST equation of state model at 45 °C and 0.10 MPa.[3] [d]Derived cetane number measured at NREL using ASTM D6890 unless noted otherwise. [e]Lower heating value (i.e., net heat of combustion). [f]2,2,4,4,6,8,8-heptamethylnonane (aka isocetane). [g]Defined value.

DOI: 10.1021/acs.energyfuels.5b02879
Energy Fuels 2016, 30, 1445−1461

Table 3. Surrogate-Fuel Compositions

	V0a (4-comp.)		V0b (5-comp.)		V1 (8-comp.)		V2 (9-comp.)	
Palette Compound Abbrev.	mol %	wt %	mol %	wt %	mol %	wt %	mol %	wt %
NHXD	27.8	32.2	0	0	2.7	3.2	0	0
NOD	0	0	23.5	32.1	20.2	27.3	10.8	15.2
NEI	0	0	0	0	0	0	0.8	1.2
HMN	36.3	42.0	27.0	32.8	29.2	35.1	0	0
2MHPD	0	0	0	0	0	0	7.3	10.2
NBCX	0	0	0	0	5.1	3.8	19.1	14.8
TIPCX	0	0	0	0	0	0	11.0	12.8
TDEC	14.8	10.5	0	0	5.5	4.0	0	0
PHP	0	0	0	0	0	0	6.0	6.4
TMB	0	0	12.5	8.1	7.5	4.8	0	0
TIPB	0	0	0	0	0	0	14.7	16.6
TET	0	0	20.9	14.8	15.4	10.8	16.4	12.0
1MN	21.1	15.3	16.1	12.3	14.4	10.9	13.9	10.9

section 3.3 of our previous work, except that the palette compounds and weighting factors were different, and no limits were imposed on the mole fractions of CT9 or CT10 in the current research. The final weighting factors on CT, DCN, ADC points, and density that were used in the regression model to formulate the various surrogates are provided in the Supporting Information in Table S2. The surrogate-fuel compositions determined using this approach are provided in Table 3.

2.4. Palette-Compound Procurement, Safe Handling, Analysis, Treatment, and Additization. A great deal of effort was expended in obtaining and characterizing high-purity, ultralow-sulfur palette compounds to establish a strong foundation for the research community to formulate high-quality diesel surrogate fuels. High-purity palette compounds were desired to minimize the uncertainties in ignition quality, emissions, and other performance characteristics introduced by unknown impurities. The ultralow-sulfur levels support the objectives that these surrogate fuels should (1) have sulfur levels consistent with those found in commercial on-road diesel fuels, and hence be compatible with sulfur-sensitive exhaust-gas aftertreatment systems; and (2) not require a more-complicated interpretation of particulate-matter emissions results due to the presence of sulfate in the exhaust stream.

2.4.1. Procurement. Many compounds were easily procured from well-known chemical suppliers, but some of the palette compounds had to be obtained by custom synthesis and/or purification. The palette compounds and their sources are provided in Table 4. Of these, the procurement of ultralow-sulfur, high-purity 1-methylnaphthalene (1MN) was particularly challenging. As shown in Table 3, 1MN is found in all four surrogates. It is the only commonly available palette compound with a boiling point in the middle of the typical diesel boiling range that is also representative of compounds found in commercial diesel fuels. Unfortunately, analyses of samples from domestic and international suppliers showed that commercially available 1MN generally has relatively low purity (~95 wt %) and high sulfur levels (5000−20000 ppmw), so significant effort was required to develop a source of >98 wt % purity, <15 ppmw sulfur 1MN. Approximately 10 purification and custom-synthesis approaches were explored to achieve these specifications, and a successful source is included in Table 4.

2.4.2. Safety and Handling. Established chemical-safety guidelines[66] should be followed when handling and using any of the palette compounds and fuels described in this research. In addition, some of the palette compounds pose special hazards. TDEC and TET are known peroxide-forming compounds,[67,68] and 1MN is sufficiently toxic that its Safety Data Sheet (SDS) recommends the use of a full-face respirator during handling.[69] Given the structural similarities between TDEC and PHP, it is advisable to treat PHP as a peroxide-forming compound as well. A thorough treatment of palette-compound hazards is outside the scope of this research; hence, the user is encouraged to read the SDSs for all of the palette compounds before working with them or their mixtures. Filling the headspaces of fuel containers with nitrogen is also recommended to inhibit peroxide formation during storage and use.

Table 4. Palette-Compound Procurement Information[a]

palette compd abbrev	supplier[b]	product no.	purity (wt %) stated	purity (wt %) measd[d]	approx cost[e] ($/kg)
NHXD	FS	AC120460100	99	99.1	160
NOD	SA	O652	99	99.3	370
NEI	SA	219274	99	98.9	390
HMN	FS	AC156250010	98	99.1	470
2MHPD	ES	CS[c]	≥ 98	98.5	5000
NBCX	TCI	B0822	>99	99.8	840
TIPCX	SA	H (from TIPB)[c]	≥98	98.6	4590
TDEC	TCI	D0007	>98	99.5	550
PHP	SA	H (from PA)[c]	≥98	98.7	8910
TMB	FS	50−700−0019	98	99.2	30
TIPB	SA	CS[c]	≥98	98.1	1990
TET	SA	522651	99	99.2	100
1MN	ES	P[c]	≥98	99.5	4000

[a]Commercial equipment, instruments, or materials are identified only in order to adequately specify certain procedures. In no case does such identification imply recommendation or endorsement by the National Institute of Standards and Technology, nor does it imply that the products identified are necessarily the best available for the purpose. [b]ES = Eastern Sources,[60] FS = Fisher Scientific,[61] SA = Sigma-Aldrich,[62] and TCI = TCI America.[63] [c]CS = custom synthesis, H = hydrogenation, P = purification, and PA = phenanthrene. [d]Measured at CanmetENERGY by GC×GC-FID.[64,65] [e]For estimation purposes only, in 2014 U.S. dollars. Rounded to nearest $10. Costs for nonstock items may include supplier development costs.

2.4.3. Initial Analyses. Upon receipt from the supplier, the purity and sulfur content of each batch of each palette compound were verified by GC×GC-FID[70] (for purity) as well as ASTM D5453[71] and/or GC×GC-SCD[70] (for sulfur content). In addition, DCNs were measured for palette compounds with previously unknown ignition qualities.[43]

2.4.4. Silica-Gel Treatment. Each palette compound was treated with activated silica gel to remove peroxides (and/or other polar contaminants), using a procedure similar to that reported by Wallace and Renz.[33] The silica gel was activated by heating in a muffle furnace at 250 °C for about 60 h, after which it was cooled, and a column of 100 g was loaded into a buret. This column was used to treat up to 1050 g of a given palette compound (or mixture of palette compounds) by gravity drainage, after which the silica gel was

DOI: 10.1021/acs.energyfuels.5b02879
Energy Fuels 2016, 30, 1445−1461

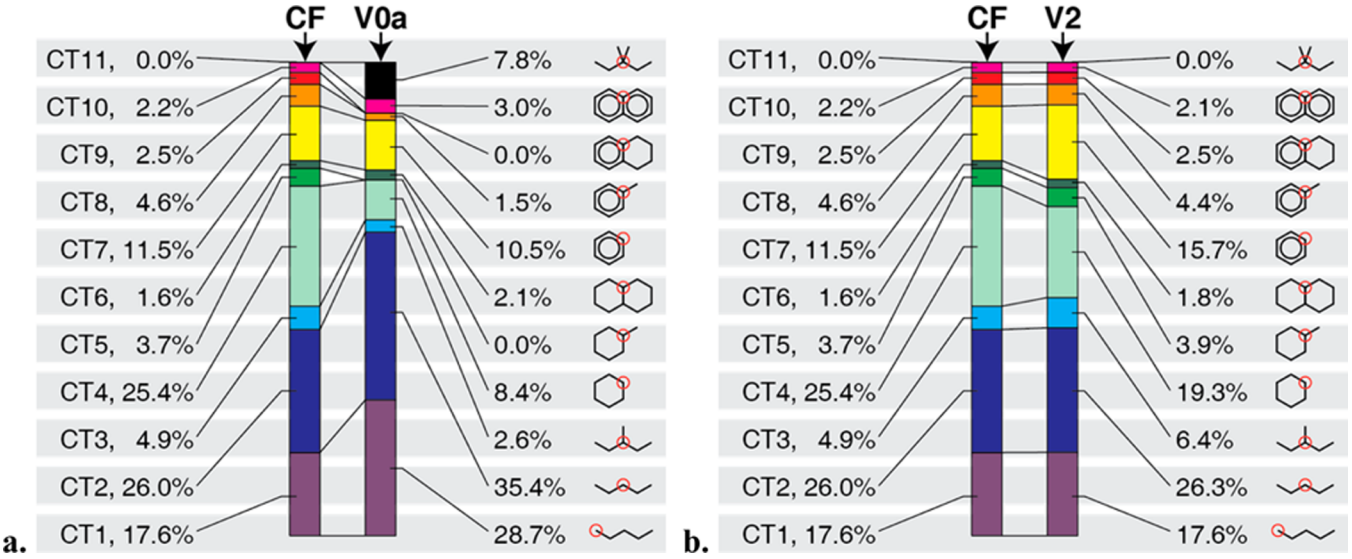

Figure 3. CT mole fractions for CF target fuel (as quantified by NMR spectroscopy, left-hand vertical bar of each pair) vs CT mole fractions determined from known surrogate composition (right-hand vertical bar of each pair): (a) V0a surrogate; (b) V2 surrogate. Each gray horizontal bar in the background corresponds to a numbered CT, and a structural diagram with the given CT circled in red is provided near the right-hand end of each bar for reference.

replaced with a fresh batch. The low space velocities afforded by gravity drainage were found to be critical for effective peroxide removal. Just under 10% of each palette compound was lost due to being retained in the column after silica-gel treatment (SGT).

The aforementioned treatment was applied to most of the palette compounds in their pure forms, rather than to the fully blended surrogate fuels. Although this approach was more labor-intensive, it was employed due to experimental evidence that more-polar/polarizable compounds tend to be preferentially adsorbed to the silica gel, which can change the composition of a fuel blend, particularly for blends of nonpolar compounds (e.g., alkanes) with polarizable compounds (e.g., aromatics). The preferential removal of low-DCN aromatic compounds could help explain why SGT of two blended surrogate fuels failed to lower the measured DCNs to expected values in a prior study (see Figure 13 of our previous paper[25]). SGT was not applied to the CF target fuel for this reason. The potential for preferential adsorption during SGT provides another motivation for using surrogate fuels; namely, once the target fuel contains peroxides, it may not be possible to remove those peroxides without also altering the target-fuel composition.

SGT as described previously could not be conducted on the two heaviest *n*-alkanes (NOD and NEI) individually because they are solids at room temperature. Instead, these compounds were first dissolved in either HMN (for V0b and V1) or 2MHPD (for V2), and then these solutions were treated in columns packed with baked silica gel as described earlier, but heated to about 50 °C to prevent solidification (and hence loss) of NOD or NEI in the columns.

Upon receipt from their respective suppliers, the pure palette compounds had peroxide levels ranging from ~2 to 3 ppm (for HMN, TDEC, and NBCX) to 95 ppm (for TMB). After SGT, the peroxide levels of all palette compounds fell within the range of 0−11 ppm.

2.4.5. Additization. Each palette compound was individually additized to inhibit its oxidation rate and to improve its lubricity. The antioxidant (AO) used was a hindered phenol (Nalco EC5208A), and it was added at a treat rate of 100 ppmw. The AO was added immediately following SGT because it does not remove peroxides that are already present; it simply inhibits the formation of new peroxides. The lubricity improver (LI) used was Infineum R696, and it was added at a treat rate of 150 ppmw. The total AO and LI treat rates by mass in the surrogate fuels are identical to those in the individual palette compounds because the AO and LI mass fractions were held constant in all of the palette compounds. The AO and LI[72] additives are not expected to change the ignition quality of their base fuel beyond the uncertainty limits of the ASTM D6890 test method for DCN because the additives are not peroxides and they were added at such a low level (250 ppmw total = 0.025 wt %).

2.5. Surrogate-Fuel Blending. The surrogate fuels were not blended until after purity, sulfur, and DCN analyses, SGT, and the addition of AO and LI. Approximately 30 L of each surrogate fuel was blended by adding the desired mass of each component to a container and mixing. Proper blending was verified by GC×GC-FID analysis of the finished surrogate fuels.

3. PHYSICAL AND CHEMICAL PROPERTY TESTING OF TARGET AND SURROGATE FUELS

Once the surrogate fuels were blended, their chemical and physical properties were characterized. Results from analyses of the surrogate-design properties of composition, ignition quality, volatility, and density are presented first, followed by results for a number of other properties that were not explicitly matched between the target and surrogate fuels.

3.1. Composition. Target- and surrogate-fuel compositions were quantified in terms of CT mole fractions and hydrocarbon-class mass fractions.

3.1.1. CT Mole Fractions. Figure 3 shows comparisons between the CT mole fractions in the CF target fuel (as quantified by NMR spectroscopy, described in section 2.1.2) vs CT mole fractions in the V0a and V2 surrogates (as calculated from their known compositions). A quick visual comparison of the stacked vertical bar graphs in Figure 3a,b shows that, as expected, the V2 surrogate provides a closer match to the target fuel than the V0a surrogate. The V2 surrogate contains all of the CTs identified in CF with a 1.2 mol % average absolute difference across all CTs. In contrast, the V0a surrogate does not contain CTs 5 or 9 that were identified in CF, it does contain CT11 that was not found in CF, and it has a significantly larger (5.4 mol %) average absolute difference across all CTs. Corresponding graphs for the V0b and V1 surrogates are provided in the Supporting Information as Figure S3a,b, and their average absolute differences across all CTs are 5.1 and 4.5 mol %, respectively. This indicates that the compositional accuracy relative to the CF target fuel, as

DOI: 10.1021/acs.energyfuels.5b02879
Energy Fuels 2016, 30, 1445−1461

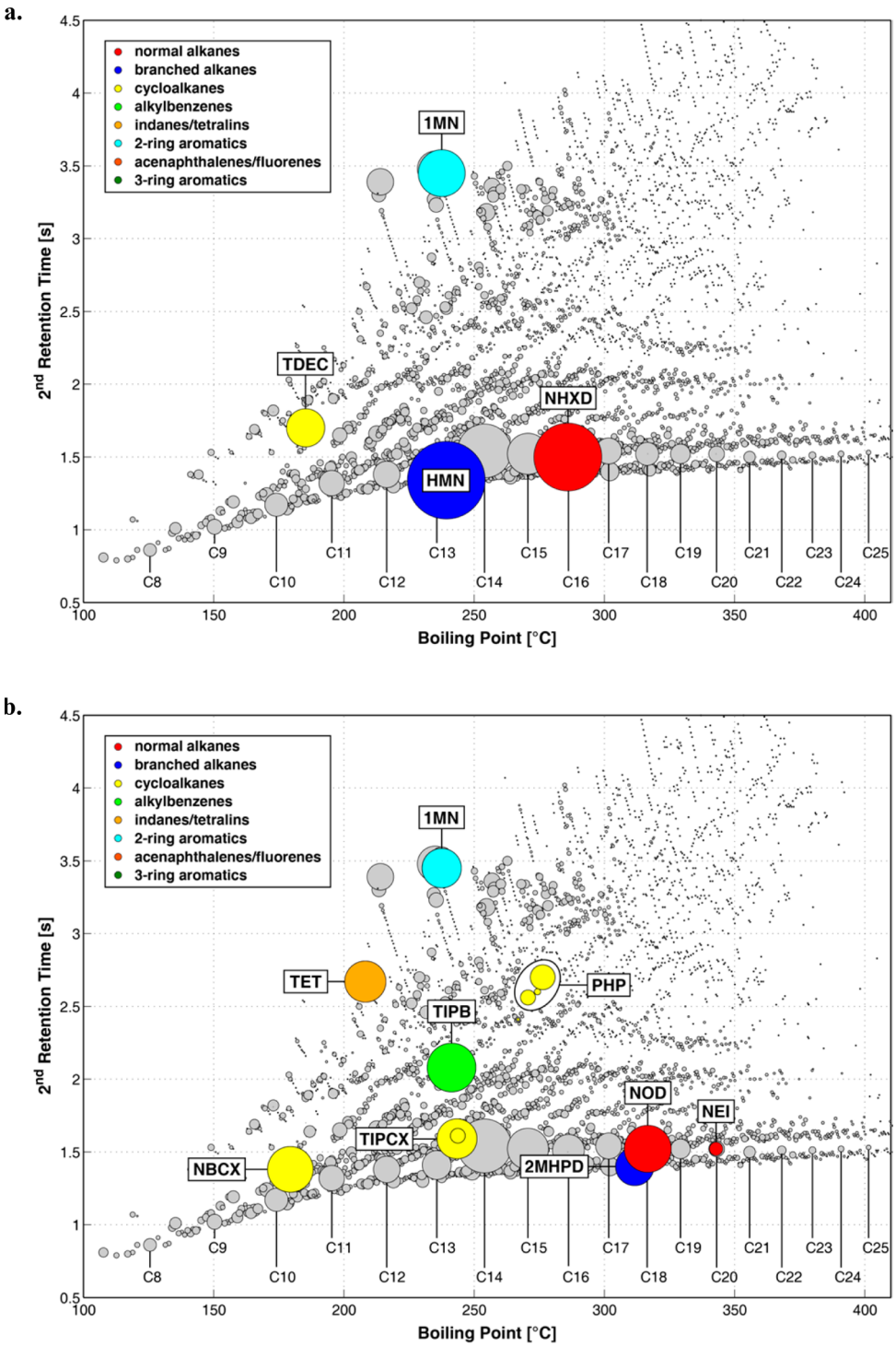

Figure 4. GC×GC-FID chromatograms acquired with the "normal" column configuration, showing surrogate palette compounds (in color and labeled) overlaid on CF target-fuel composition (in gray): (a) V0a surrogate; (b) V2 surrogate. The area and color of the circle for each palette compound/isomer correspond to its mass fraction and hydrocarbon class, respectively. The individual isomers of TIPCX and PHP are evident in the chromatogram for the V2 surrogate. Annotations showing the carbon numbers and boiling points of the individual *n*-alkanes are provided for reference.

quantified by CT mole fraction, increases from V0a → V0b → V1 → V2, as expected.

3.1.2. Hydrocarbon-Class Mass Fractions. Panels a and b of Figure 4 show GC×GC-FID chromatograms acquired for the V0a and V2 surrogates, respectively, using the normal-column configuration. Using a convention similar to that in Figure 1, the palette compounds found in each surrogate are indicated by labeled, colored circles, with the area and color of each circle corresponding to the mass fraction and hydrocarbon class, respectively, of the compound. The gray circles in the background show the composition of the CF target fuel, for reference. Panels a and b of Figure S4 in the Supporting Information are the corresponding plots for the V0b and V1 surrogates, respectively.

DOI: 10.1021/acs.energyfuels.5b02879
Energy Fuels 2016, 30, 1445−1461

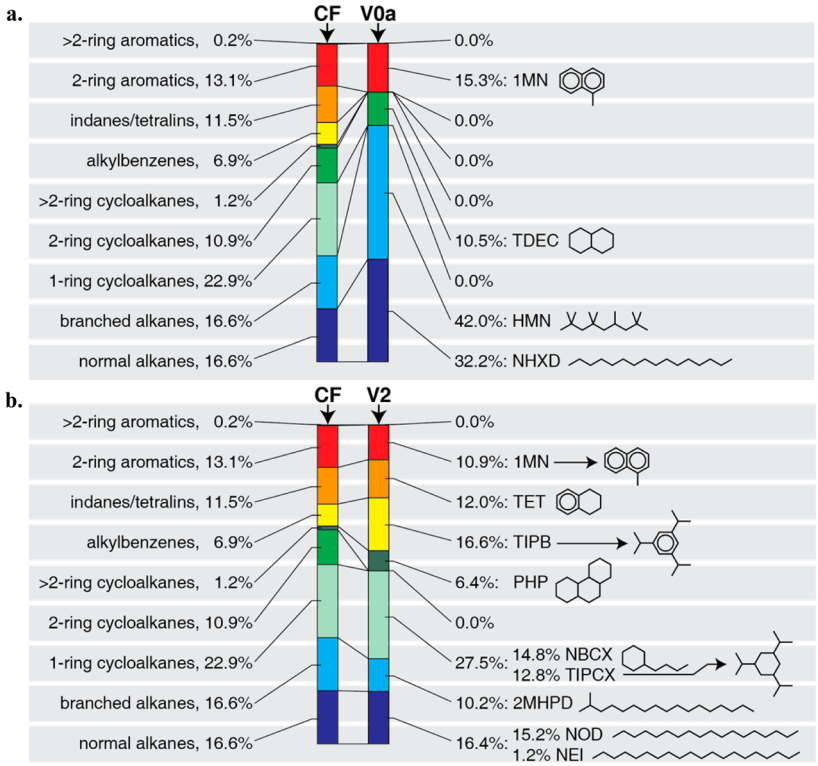

Figure 5. Hydrocarbon-class mass fractions in target fuel (left side, as quantified by GC×GC-FID) vs surrogate fuel (right side, from known surrogate composition): (a) V0a surrogate; (b) V2 surrogate.

From Figure 4a, it is evident that each palette compound in V0a falls into one of two general categories: highly polar/polarizable (long retention time along the *y*-axis) or highly nonpolar (short retention time along the *y*-axis) for its given boiling point (position on the *x*-axis). As shown in the Supporting Information (Figure S4), surrogates V0b and V1 have chromatograms similar to that of V0a and are thus composed of palette compounds representing either high or low polarizability for their given boiling points, but not intermediate. In contrast, Figure 4b shows that the V2 palette compounds exhibit a wider range of polarizability at their given boiling points, demonstrated by intermediate retention times in the *y*-dimension, due to the inclusion of TIPB and PHP. As a result, the V2 surrogate better covers the area of the CF chromatogram than the other surrogates.

Comparison of Figure 4b with Figure 1 reveals that most of the palette compounds elute into the expected regions identified in the CF chromatogram (i.e., their retention times in the GC columns place them within expected regions based on observations for similar compounds within the same hydrocarbon class), but the PHP isomers are found in the "indanes/tetralins" rather than the "cycloalkanes" region of the chromatogram. This is a good example of hydrocarbon-class assignments being challenging for some compounds due to overlapping elution times. As shown in Supporting Information Figure S1b, the PHP isomers correctly fall within the " >2-ring cycloalkanes" region of the GC×GC chromatogram when the reverse-column configuration is employed, which was one motivation for using the reverse-column configuration.

Figure 5 provides comparisons between the hydrocarbon-class mass fractions in the CF target fuel (as quantified by GC×GC-FID, described in section 2.1.1) vs the hydrocarbon-class mass fractions in the V0a and V2 surrogates (as determined from their known compositions). The corresponding graphics for the V0b and V1 surrogates are provided in the Supporting Information as Figure S5. Whereas the V0a surrogate contains only four of the nine hydrocarbon classes specified in Figure 5, the V2 surrogate contains seven. The V0b and V1 surrogates contain five and seven of the specified classes, respectively. Although CT mole fractions were chosen as the composition-design parameter rather than hydrocarbon-class mass fractions, the hydrocarbon-class mass fractions of the higher-accuracy surrogates also more closely match those of the target fuel, as expected. The absolute differences between the CF target fuel and the surrogates, averaged over the nine specified hydrocarbon classes, are 9.6, 8.0, 7.2, and 4.4 wt %, respectively, for the V0a, V0b, V1, and V2 surrogates. In other words, the compositional accuracy with respect to the CF target fuel increases from V0a → V0b → V1 → V2, as expected.

3.2. Ignition Quality. Figure 6 shows the ignition quality of the CF target fuel and each of the surrogate fuels as quantified by DCN (i.e., ASTM D6890[55]), as well as the DCN for each surrogate fuel as predicted by a volume-fraction-weighted linear blending rule (eq 4 in our previous paper[25]) employing the DCNs of the palette compounds provided in Table 1. For CF, both bars represent measured values, with the left-hand bar representing the average of measurements from 2009 to 2011 reported in previous work,[25] and the right-hand bar representing the average value measured in October 2014. The DCNs for the surrogate fuels were all measured during the last quarter of 2014 as well. For the surrogate-fuel measurements conducted in 2014, the left-hand, non-cross-hatched bar in each pair represents the average of two replicates. The greatest difference between the two replicates was 0.3 DCN (for V2), which is significantly better than the stated repeatability of the technique. The measured values of all of

DOI: 10.1021/acs.energyfuels.5b02879
Energy Fuels 2016, 30, 1445−1461

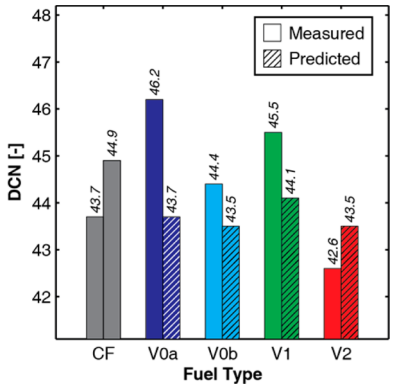

Figure 6. Target- and surrogate-fuel ignition qualities as quantified by derived cetane number (DCN)[55] or estimated using a volume-fraction-weighted linear blending rule.[25]

the surrogates match the average DCN of CF within the ±2.85 reproducibility of the technique for a 45-DCN fuel.[55] V0a has the largest positive deviation (+1.9) relative to the CF average (44.3), whereas V2 has the largest negative deviation (−1.7). The DCN for V1 has a deviation of 1.2, and V0b has the smallest deviation at 0.1.

All of the predicted values for the surrogates are tightly clustered near the low end of the measured DCN range for CF. This is expected because the older DCN value for CF of 43.7 was used as the target value in the regression model when the surrogate-fuel formulations were determined. Comparing predicted to measured values for the surrogates, the measured values are higher for all of the surrogates except V2.

Based on previous work showing that ignition-accelerating contaminants (likely peroxides) could form in fuels over time, and their presence at levels of ∼10 ppm could noticeably affect DCN values,[25,33] the peroxide contents of the fuels were measured in 2014 using a proprietary method developed at Chevron. These results are shown in Figure 7. The relatively

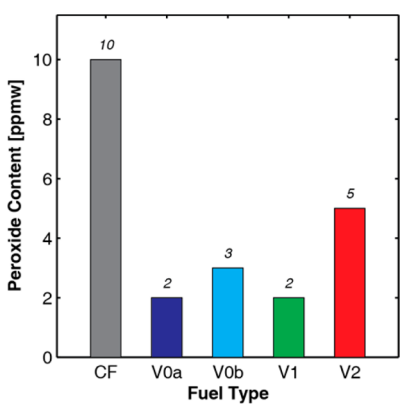

Figure 7. Target- and surrogate-fuel peroxide contents.

higher peroxide content of CF may be due to a buildup of peroxides over time because it is the oldest fuel, and SGT was not performed on CF due to concerns that this could affect its composition (see section 2.4.4). Although peroxide measurements were not made for CF in 2009, a slow increase in peroxide content could help explain the slowly increasing DCN of CF with time evident in Figure 6. The relatively higher peroxide content of V2 and it being the only surrogate with a measured DCN less than its predicted DCN suggest that at least one of the DCNs for the V2 palette compounds could be too low (see section 3.5.2 of our previous paper[25] for a discussion of uncertainties in palette-compound DCNs), or that a more-sophisticated blending model featuring blend factors may be beneficial.[73]

3.3. Volatility. Target- and surrogate-fuel volatilities were quantified using the advanced distillation curve technique[56−58] as well as simulated distillation (ASTM D2887)[74] and standard distillation (ASTM D86)[75] techniques.

3.3.1. Advanced Distillation Curve. ADC distillation points were used in the regression model for matching the volatilities of the target and surrogate fuels. Figure 8 shows the ADC data as measured for the CF target fuel, as measured and predicted for the V0a and V2 surrogates, and the differences between the measured values for the target fuel and the V0a and V2 surrogates. Figure S8 in the Supporting Information provides the corresponding information for the V0b and V1 surrogates. The details of the ADC measurements, including determination of the enthalpy of combustion as a function of distillate fraction and uncertainty analyses, are provided in Burger et al.[76]

The simple, four-component V0a surrogate provides the poorest match to the ADC of the CF target fuel, a trend that is also found when volatility is quantified using the simulated distillation[74] or standard distillation[75] test methods (see sections 3.3.2 and 3.3.3, respectively). V0a is not volatile enough at the light end of the distillation range, but above T20 (the temperature at which 20 vol % of the fuel has been recovered) V0a transitions to being too volatile, with the mismatch increasing toward the heavy end of the distillation curve. All of the surrogates are more volatile than the target fuel at the heavy end of the distillation curve (T80 and higher), though to a lesser extent than observed with V0a. This mismatch is likely to result in shorter in-cylinder liquid-phase fuel penetration lengths (i.e., liquid lengths) for V0a relative to those of CF, because liquid lengths have been shown to correlate well with the heavy end of the fuel distillation range.[77,78]

The V0b, V1, and V2 surrogates all provide reasonable matches to the measured ADC of CF, with V0b featuring the smallest absolute difference averaged over the measured distillation range (the average absolute differences between the measured ADC points for the CF target fuel and the V0a, V0b, V1, and V2 surrogate fuels are 14.5, 4.3, 6.0, and 9.0 °C, respectively). It is interesting that the five-component V0b surrogate provides such an improved match to the ADC of CF relative to V0a, because V0b contains only one more compound than V0a. Comparing Figure 8a and Supporting Information Figure S8a indicates that the matching at the heavy end of the curve is dramatically improved for V0b. Based on palette-compound normal boiling points, it is likely that the compound responsible for the improved heavy-end matching is NOD, which is present in V0b but not in V0a. The light-end improvement likely comes from replacing TDEC with TET and TMB, both low-boiling-point components, but having values bracketing TDEC. The simulated distillation results presented in the next subsection provide further support for this hypothesis.

In general, the agreement between the measured and predicted ADC values for a given surrogate are good (i.e., within ∼5 °C) over the distillation range, with predicted ADC temperatures being systematically higher than measured values. The V2 surrogate shows poorer agreement than V0a, V0b, and V1, with predicted ADC temperatures ∼10 °C higher than

DOI: 10.1021/acs.energyfuels.5b02879
Energy Fuels 2016, 30, 1445−1461

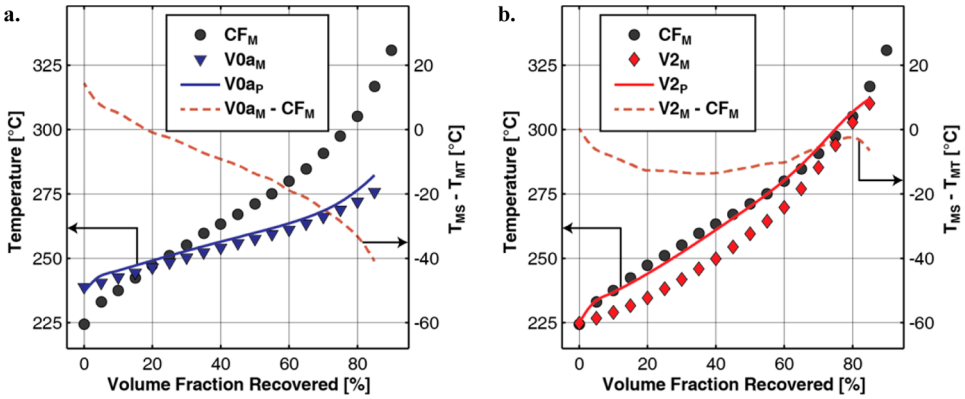

Figure 8. Fuel volatility as quantified by the ADC technique: (a) V0a surrogate; (b) V2 surrogate. Subscripts M, P, MS, and MT denote measured, predicted, measured surrogate-fuel, and measured target-fuel values, respectively.

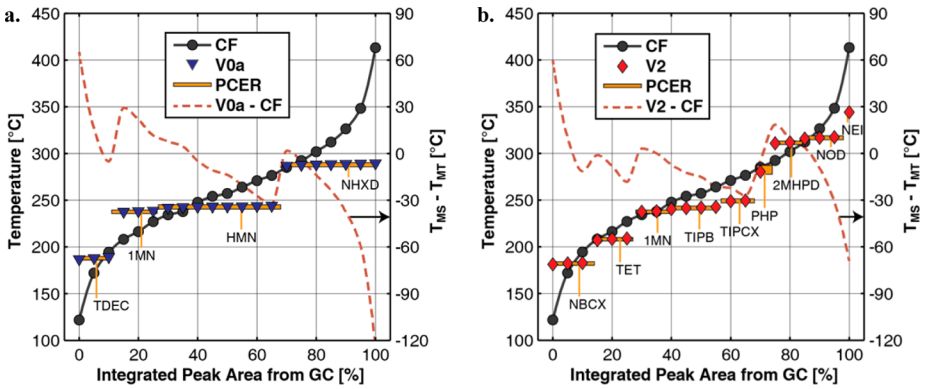

Figure 9. Fuel volatility as quantified by the simulated distillation (ASTM D2887) technique: (a) V0a surrogate; (b) V2 surrogate. Elution ranges for each palette compound (PCER) in each surrogate are shown and labeled with their corresponding palette-compound abbreviations. Subscripts MS and MT denote measured surrogate-fuel and measured target-fuel values, respectively.

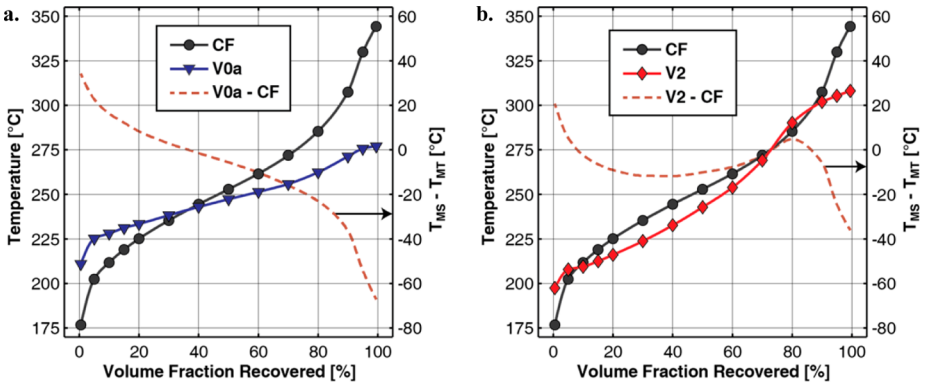

Figure 10. Fuel volatility as quantified by the standard distillation (ASTM D86) technique: (a) V0a surrogate; (b) V2 surrogate. Subscripts MS and MT denote measured surrogate-fuel and measured target-fuel values, respectively.

measured values from ~T10 to T65. This is likely due to larger uncertainties in the equations of state (EOS) for the five palette compounds that are unique to V2. In particular, there were very limited density, speed-of-sound, heat-capacity, and vapor-pressure data available to construct accurate EOS for TIPB and PHP at the time the predicted ADC data were calculated, and the model for predicting the ADC is known to be especially sensitive to the vapor-pressure data used to construct the EOS for each palette compound.

3.3.2. Simulated Distillation. Figure 9 shows simulated distillation (ASTM D2887[74]) data as measured for the CF target fuel and the V0a and V2 surrogates, the measured palette-compound elution range (PCER) for each palette compound in each surrogate, and the differences between the measured values for the target fuel and the V0a and V2 surrogates. Figure S9 in the Supporting Information provides the corresponding information for the V0b and V1 surrogates. Simulated distillation is a gas-chromatography-based method that simulates the distillation process via measured elution times through a column.[74]

As was observed in the ADC results, V0a provides the poorest match to the target-fuel distillation characteristics, being too heavy at the light end of the distillation curve and too light at the heavy end. Whereas measured ADC data are

DOI: 10.1021/acs.energyfuels.5b02879
Energy Fuels 2016, 30, 1445−1461

available to T85 for the surrogates, the D2887 measurements are available to T100. The D2887 data indicate that the trend of poorer matching between V0a and CF continues to worsen all the way to T100. Also, as was evident from the ADC results, there is a comparable degree of matching between the target fuel and the V0b, V1, and V2 surrogates, but the magnitudes of the target-vs-surrogate temperature differences are larger when quantified using the D2887 method.

In contrast to the ADC method, the D2887 method yields plateau regions that correspond to individual palette compounds, giving the D2887 distillation profiles a stair-step shape for the surrogates (also see, e.g., Figures 6 and 7 of Reiter et al.[4]). The PCERs in Figure 9 and Supporting Information Figure S9 provide additional valuable information regarding when each palette compound elutes as the D2887 procedure is conducted. For example, comparison of Figure 9a and Supporting Information Figure S9a lends further support to the hypothesis that it is the inclusion of NOD in the V0b palette that leads to the improved target-fuel matching at the heavy end of the distillation curve. In general, the palette compounds elute in order of increasing normal boiling point. As was evident in the ADC results, all of the surrogates have distillation temperatures that are too high at the light end of the distillation range and too low at the heavy end (relative to the CF target fuel).

3.3.3. Standard Distillation. To facilitate comparisons of ADC and simulated distillation results with the industry-standard volatility-quantification technique, Figure 10 shows standard distillation (ASTM D86)[75] data as measured for the CF target fuel and the V0a and V2 surrogates, as well as the differences between the measured values for the target fuel and the V0a and V2 surrogates. Figure S10 in the Supporting Information provides the corresponding information for the V0b and V1 surrogates.

The same general volatility trends are observed as were evident using the other methods, namely, the following: V0a exhibits the poorest matching to the CF target fuel; the V0b, V1, and V2 surrogates show comparable matching; and all of the surrogates have distillation temperatures that are too high at the light end of the distillation range and too low at the heavy end (relative to the target fuel). This general agreement is noteworthy given that the ranges and absolute values of the distillation temperatures determined from the ADC, simulated distillation, and standard distillation techniques show such significant differences.

3.4. Density. Target- and surrogate-fuel densities at 20 °C were quantified using the ASTM D4052 method,[59] and surrogate-fuel densities at 20 °C were estimated using an EOS-based method developed at NIST.[3] The results are shown in Figure 11. It is evident from the measured values that V2 provides the closest match to the target-fuel density (within <1%), which is expected because one criterion for selecting the new compounds in the V2 palette was that they have densities more representative of compounds found in the target fuel. V0b provides the next-best match, followed by V1 and then V0a. All of the measured surrogate-fuel densities fall within 3.4% of the target-fuel density. The predicted density for each surrogate is 1−2% lower than its corresponding measured value, presumably due to incomplete information on palette-compound properties and mixture parameters.

3.5. Other Properties. A number of additional properties of the target and surrogate fuels were measured to assist in further assessing the soundness of the current surrogate-formulation methodology as well as the suitability of the surrogate fuels for testing in engines and other experimental setups.

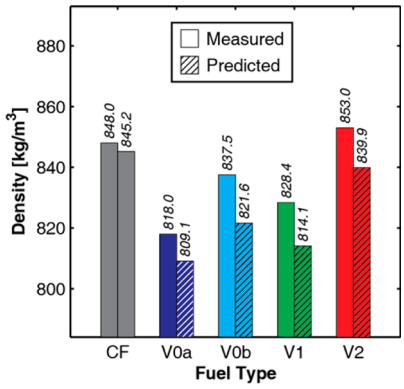

Figure 11. Measured target-fuel densities, as well as measured and predicted surrogate-fuel densities at 20 °C and ∼0.1 MPa ambient pressure. For CF, both bars represent measured values, with the left- and right-hand bars corresponding to measurements made by different testing laboratories in 2009 and 2014, respectively. Each non-cross-hatched bar represents a single measurement acquired per the ASTM D4052 test method.[59]

3.5.1. Net Heat of Combustion. The net heats of combustion for the target and surrogate fuels were quantified using ASTM D4809.[79] In addition, the net heats of combustion (aka lower heating values, LHVs) for the surrogate fuels were estimated from the net heats of combustion of their constituent palette compounds shown in Table 1 and the known compositions of the surrogate fuels using a mass-fraction-weighted linear-blending rule. The measured and estimated values are presented in Figure 12. All values agree with the average measurement for the target fuel within a tolerance of ±1%.

3.5.2. Lubricity. The lubricity of the target fuel was measured using ASTM D6079[80] (high-frequency reciprocating rig), as were the lubricities of the surrogate fuels before and after addition of lubricity improver (LI; see section 2.4.5). The results shown in Figure 13 indicate that none of the surrogate fuels met the maximum wear-scar diameter of 520 μm per the

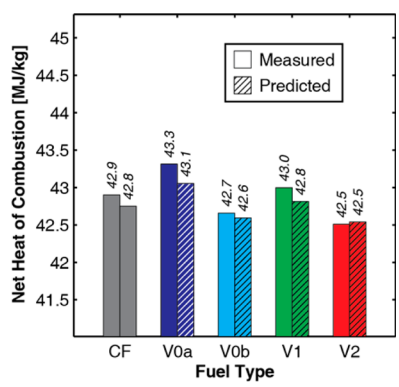

Figure 12. Measured target-fuel net heats of combustion, as well as measured and predicted surrogate-fuel net heats of combustion. For CF, both bars represent measured values, with the left- and right-hand bars corresponding to measurements made by different testing laboratories in 2009 and 2014, respectively. Each non-cross-hatched bar represents a single measurement acquired per the ASTM D4809 test method.[79]

DOI: 10.1021/acs.energyfuels.5b02879
Energy Fuels 2016, 30, 1445−1461

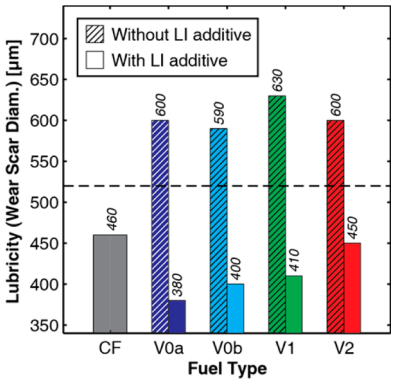

Figure 13. Target- and surrogate-fuel lubricities measured using ASTM D6079.[80] Each bar represents a single measurement acquired per the test method. Dashed line indicates the maximum wear-scar diameter of 520 μm for grade no. 2-D S15 diesel fuel from the ASTM D975 specification. A small batch of each surrogate fuel created without LI additive was tested to give the values shown by the cross-hatched bars. As indicated in Table S1 of the Supporting Information, CF was provided with LI already added, and no further LI was added to this fuel.

ASTM D975 specification for grade no. 2-D S15 diesel fuel[30] prior to addition of the LI, but all of them met the specification after additization.

3.5.3. Cloud Point and Final Melting Point. The cloud points and final melting points of the fuels in this study were quantified using ASTM D5773[81] and a similar procedure developed at NREL,[82] respectively. The measurements were made at constant cooling/heating rates of magnitude 1.5 °C/min at ~0.1 MPa ambient pressure. The cloud point (CP) is the temperature at which, as the fuel temperature is lowered, crystals of solidified fuel become visible. The final melting point (FMP) is the temperature at which, as the fuel temperature is raised, the last crystals of solidified fuel disappear. From a low-temperature performance perspective, it is desirable to have CPs and FMPs as low as possible, because crystals/waxes in the fuel can plug fuel filters and cause fuel-injection system malfunctions.

The measured CPs and FMPs for the fuels in this study are provided in Figure 14. It is clear that the CF target fuel has the most-desirable low-temperature performance characteristics,

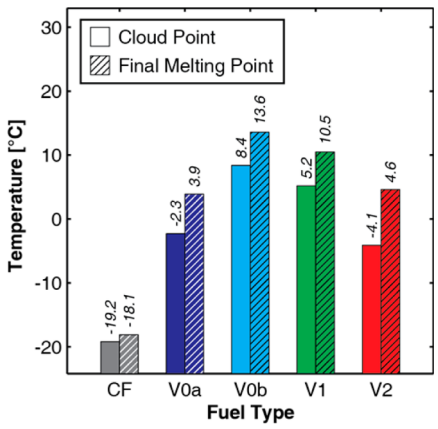

Figure 14. Target- and surrogate-fuel cloud points and final melting points. Each bar represents a single measurement acquired per the corresponding test method (at ~0.1 MPa ambient pressure).

followed by V2 and V0a (which have comparable performance), then V1, and finally V0b. It is also evident that the FMP for a given fuel is always higher than its CP; i.e., the temperature at which solids first appear as the fuel is cooled is colder than the temperature at which solids disappear as the fuel is heated. This hysteresis appears to be related to difficulty in re-dissolving the crystals/waxes upon reheating of the sample.

Comparing V0a and V0b, it is noteworthy that the improved matching at the heavy end of the distillation curve afforded by the addition of NOD to V0b comes at the expense of low-temperature performance, where V0b is clearly inferior to V0a. (It has been verified by GC that the first-to-solidify material in V0b is NOD.) It is also interesting that although V2 contains both NOD and the heavier *n*-alkane NEI, it has low-temperature performance similar to V0a, which contains no *n*-alkanes heavier than NHXD. V2 also exhibits the largest difference between CP and FMP. The underlying reasons for these observations likely involve intricacies of the co-solvencies of the various palette compounds in their respective surrogate-fuel blends, a topic that is beyond the scope of this study.

3.5.3.1. Fuel Solidification at Atmospheric Pressure. The relatively high (even close to room temperature for V0b) CPs and FMPs of the surrogates provided an initial indication that care needs to be taken to minimize the effects of fuel solidification when storing and testing the surrogates at atmospheric pressure. It is recommended that the surrogates be simultaneously warmed to at least 16 °C and stirred before and during use, to melt any crystallites and ensure mixture homogeneity, respectively.

3.5.3.2. Fuel Solidification at Elevated Pressures. Subsequent measurements at elevated pressures typical of those present in modern common-rail fuel-injection systems showed that fuel solidification occurs at even higher temperatures for the surrogates, with FMP increasing approximately linearly with pressure. For example, at 250 MPa rail pressure, a fuel temperature of ~80 °C (conservative estimate) is required to keep all of the surrogates in the liquid phase. In contrast to the behavior of the surrogates, the FMP for CF appears to remain approximately constant at its atmospheric-pressure value to at least 250 MPa.

For high-pressure testing of the surrogates, it is recommended that all of the high-pressure components of the fuel system be maintained at a sufficiently high temperature to avoid solidification. A possible alternative to heating the fuel system would be to add a cold-flow improver to each surrogate. In either case, careful attention should be paid to ensure that no fuel solidification occurs during experimental testing.

3.5.4. Elemental Analysis. The carbon and hydrogen mass fractions of all of the fuels used in this study were quantified using ASTM D5291.[35] These values are shown in Figure 15, as well as the carbon and hydrogen mass fractions of the surrogate fuels that would be expected based on their known compositions. Excellent agreement is evident in that the measured values for the surrogate fuels all fall within 1% (abs) of the measured value for the target fuel and within 0.4% (abs) of their predicted values.

3.5.5. Smoke Point. The smoke points of all of the fuels used in this study were measured using the ASTM D1322[83] test method, and the resultant values are presented in Figure 16. The smoke point and parameters based on the smoke point are used to estimate the sooting propensities of jet fuels, with a lower smoke point indicating a greater propensity to form soot.

DOI: 10.1021/acs.energyfuels.5b02879
Energy Fuels 2016, 30, 1445−1461

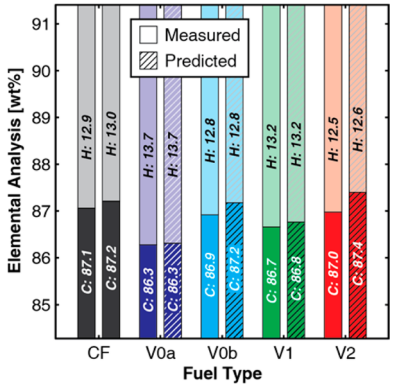

Figure 15. Target- and surrogate-fuel carbon and hydrogen mass fractions. Measured values represent a single replicate determined using ASTM D5291,[35] whereas predicted values were determined using the known compositions of the surrogate fuels. The two columns for the CF target fuel correspond to measurements made in 2009 (left-hand side) and 2015 (right-hand side). Some of the measured values do not sum to 100.0 wt % because this is not a requirement of the test method.

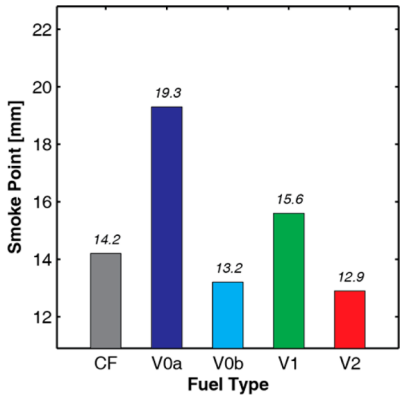

Figure 16. Target- and surrogate-fuel smoke points as measured using the ASTM D1322 test method.[83] The value for CF is an average of measurements of 13.4 and 15.0 mm from 2011 and 2014, respectively. The values for the surrogate fuels are from single replicates of the test method.

Based on the results in Figure 16 alone and if the smoke point is well-correlated with soot emissions under diesel-combustion conditions, then V0b would be expected to best match the soot emissions of the CF target fuel, followed by V1 and V2 (which should provide a similar match to CF but with V1 producing less soot than V2), and finally V0a providing the poorest agreement with CF and the lowest soot levels. It will be interesting to see whether these trends are confirmed in engine, combustion-vessel, and other experiments.

3.5.6. Other Measured Fuel Properties: Sulfur Content, Flash Point, Corrosivity, Kinematic Viscosity, Aromatic Content, and Surface Tension. Table 5 provides the values of these properties for the CF target fuel and each of the surrogates, as well as the method by which each property was quantified, except for surface tension (the measurement procedure for which is described in the following paragraph). The ASTM D975 specification for grade no. 2-D S15 diesel fuel[30] requires <15 ppmw sulfur, >52 °C flash point, corrosivity better than no. 3, and kinematic viscosity at 40 °C between 1.9 and 4.1 cSt (note, 1 cSt = 10^{-6} m^2/s). Table 5 shows that CF and each of its surrogate fuels conform to these limits, with considerable margins. The ASTM D975 specification does not limit aromatic content as measured by ASTM D5186.[84] Rather, these results are included simply to show that, by comparing with the known surrogate mass fractions shown in Figure 5 and Supporting Information Figure S5, that the D5186 method is accurate to within 1.4 wt % for monoaromatics and polyaromatics in all cases except for V2 monoaromatics, where the error is a 7.4 wt % overestimation of aromatic content. The D5186 method also systematically overestimates the mass fractions of polyaromatics (i.e., 1MN) by ∼1 wt %.

3.5.6.1. Surface Tension. Table 5 shows that, in general, as the surrogate-fuel compositional accuracy increases, so does its match to the surface tension of the target fuel. The surface-tension measurements were performed using a Krüss force-balance K-12 Mk. 6 tensiometer using the "plate method" with a Wilhelmy platinum measuring plate. The sample being analyzed was held in a clean quartz sample vessel of 66.5 mm diameter and 37.5 mm height and filled to ∼80% capacity with the performance-check standard liquid or with the sample to be analyzed. The sample vessel was rigorously cleaned according to the manufacturer's recommended procedures prior to each measurement to remove chemical residues. After washing, the sample vessel and measuring plate were heated directly using a propane torch to remove any remaining organic residues. The sample vessel and measuring plate were allowed to cool to room temperature prior data acquisition. Performance checks using certified pure water and certified ethanol were conducted prior to each measurement to ensure that the instrument was

Table 5. Additional Measured Target- and Surrogate-Fuel Properties[a]

property	test method	CF	V0a	V0b	V1	V2
sulfur (ppmw)	ASTM D5453[71]	13.6	1.2	1.2	1.2	0.8
flash point (°C)	ASTM D93[85]	68	88	83	80	80
corrosivity	ASTM D130[86,b]	1A	1A	1A	1A	1A
kinematic viscosity (cSt)	ASTM D445[87,c]	2.284	2.452	2.303	2.331	2.378
aromatics by SFC[d] (wt %)	ASTM D5186[84]					
monoaromatics		19.8 {18.4}	0.1 {0.0}	24.0 {22.9}	16.5 {15.6}	36.0 {28.6}
polyaromatics		12.4 {13.3}	16.7 {15.3}	13.2 {12.3}	11.8 {10.9}	11.9 {10.9}
total aromatics		32.1 {31.7}	16.8 {15.3}	37.3 {35.2}	28.3 {26.5}	47.9 {39.5}
surface tension (mN/m)	see text	28.15 (22.9)	26.39 (23.1)	27.41 (22.8)	27.30 (22.6)	27.68 (22.7)

[a]Aromatic-content values for the CF target fuel (determined using GC×GC-FID) and the surrogate fuels (determined from known surrogate compositions) from Figure 5 and Supporting Information Figure S5 are provided in curly braces for reference. The temperature (°C) at which each surface-tension measurement was made is provided in parentheses next to the corresponding measured value. [b]3 h at 50 °C. [c]At 40 °C. [d]SFC = supercritical fluid chromatography.

DOI: 10.1021/acs.energyfuels.5b02879
Energy Fuels 2016, 30, 1445−1461

performing within the manufacturer's tolerances. Each reported measurement is the average of two separate replicates, the standard deviation of which was ≤0.05 mN/m in all cases. The temperature in °C at which each surface-tension measurement was made is provided in parentheses next to the corresponding measured value.

3.5.7. Other Calculated Fuel Properties. Additional properties required for computational modeling include the critical-point properties of the fuel and the following temperature-dependent properties at the bubble point for a liquid of the surrogate composition: pressure (analogous to the vapor pressure of a pure compound); liquid density; difference between vapor and liquid enthalpies (analogous to the heat of vaporization of a pure compound, except that the vapor has a different composition than the liquid, and liquid and vapor compositions and enthalpies will change during vaporization); and liquid heat capacity. Estimates of these properties generated using the NIST REFPROP code[3] from 20 °C to the critical temperature in 10 K increments are shown in the Supporting Information in Tables S3−S6 for the V0a, V0b, V1, and V2 surrogates, respectively. It is understood that dynamic-viscosity, thermal-conductivity, and surface-tension estimates over the same temperature range also are required as inputs for numerical simulations, and it is planned that these will be reported in a future publication.

4. SUMMARY AND CONCLUSIONS

In this research, a surrogate-fuel-formulation methodology was applied that focuses on matching compositional characteristics between target and surrogate fuels, based on the understanding that the composition of a fuel determines its properties and performance characteristics at a given engine operating condition. The diesel target-fuel composition was quantified using a hybrid approach employing NMR spectroscopy and two-dimensional gas chromatography. The compositional information was used to select surrogate palette compounds with molecular structures and weights representative of the constituents of the target diesel fuel. The palette compounds were used in a regression model to determine four surrogate-fuel formulations with increasing levels of compositional accuracy relative to the target fuel, in addition to explicit emulation of the target-fuel ignition quality, volatility, and density. High-purity, ultralow-sulfur palette compounds were procured, treated to remove peroxides, additized to inhibit oxidation and to enhance lubricity, and blended to produce ∼30 L batches of the four surrogate fuels. The surrogate compositions were verified by the techniques that were initially employed to characterize the target fuel. To assist in assessing the soundness of the current surrogate-formulation methodology as well as the suitability of the surrogate fuels for testing in engines and other experimental setups, a range of property measurements were made, including the following: ignition quality, volatility, liquid density, net heat of combustion, lubricity, cloud point, final melting point, fuel solidification at elevated pressures, elemental analysis, smoke point, sulfur content, flash point, corrosivity, kinematic viscosity, aromatic content, and surface tension. These measurements show that, in general, the more accurately a surrogate embodies the compositional characteristics of the target fuel, the more accurately it also matches the target-fuel properties. The surrogates are suitable for use in systems with modern fuel-injection equipment and sulfur-sensitive aftertreatment devices, although measures likely will be required to prevent fuel solidification at elevated pressures. Estimated values of additional surrogate thermodynamic properties (critical properties and properties along the bubble-point curve) are provided in the Supporting Information to assist researchers conducting numerical simulations with the surrogate fuels, for whom these data are required as input parameters.

The varying levels of compositional accuracy relative to the target fuel embodied by the set of surrogate fuels are intended to assist researchers in determining the minimum level of surrogate-fuel compositional accuracy required to adequately emulate the performance characteristics of the target fuel under different combustion modes. Rigorous engine and combustion-vessel testing is planned to identify which diesel surrogate fuel is indeed "as simple as possible, but not simpler," as well as to provide insights into the underlying reasons for any discrepancies between fuels. It is also planned to compare the results from the combustion testing to results from numerical simulations using the same surrogate fuels, to assist in identifying and overcoming barriers to, and ultimately enabling, accurate and cost-effective computational fuel/engine system optimization.

■ ASSOCIATED CONTENT

Supporting Information

The Supporting Information is available free of charge on the ACS Publications website at DOI: 10.1021/acs.energyfuels.5b02879.

Figures showing GC×GC-FID chromatograms, CT mole fractions, hydrocarbon-class mass fractions, and fuel volatility and tables listing manufacturer's specifications, weighting factors, and critical properties and properties along the bubble-point curve (PDF)

■ AUTHOR INFORMATION

Corresponding Author

*Phone: (925) 294-2223. Fax: (925) 294-1004. E-mail: cjmuell@sandia.gov.

Notes

The authors declare no competing financial interest.

¶R.M.G. is on leave from the University of Silesia, 40-007 Katowice, Poland.

■ ACKNOWLEDGMENTS

Funding for this research was provided by the U.S. Department of Energy (U.S. DOE) Office of Vehicle Technologies, the Coordinating Research Council (CRC) and the companies that employ the CRC members, Natural Resources Canada and the Canadian federal government interdepartmental Program of Energy Research and Development (PERD) and ecoENERGY Innovation Initiative (ecoEII), and the U.S. Army Research Laboratory. The study was conducted under the auspices of CRC. We thank U.S. DOE program managers Kevin Stork and Gurpreet Singh for supporting the participation of the U.S. national laboratories in this study. C.J.M's portion of the research was conducted at the Combustion Research Facility, Sandia National Laboratories, Livermore, CA, USA. Sandia is a multiprogram laboratory operated by Sandia Corp., a Lockheed Martin company, for the U.S. Department of Energy's National Nuclear Security Administration under Contract DE-AC04-94AL85000. W.J.C's portion of the research was funded by and conducted at Chevron Energy Technology Co., a division of Chevron USA, Richmond, CA, USA. J.T.B's portion of the

DOI: 10.1021/acs.energyfuels.5b02879
Energy Fuels 2016, 30, 1445−1461

research was conducted at Pacific Northwest National Laboratory, a multiprogram laboratory operated by the Battelle Memorial Institute under Contract No. DE-AC05-76RL01830 for the U.S. DOE. J.T.B. also thanks Drs. John Linehan, Molly O'Hagan, and Suh-Jane Lee, Mr. Gregory Coffey, Ms. Margaret Jones, Ms. Tricia Smurthwaite, and Ms. Diana Tran for their discussions and assistance in obtaining data critical to this work. W.J.P's portion of the research was performed under the auspices of the U.S. DOE by Lawrence Livermore National Laboratory under Contract DE-AC52-07NA27344. M.A.R's portion of the research was conducted at the National Renewable Energy Laboratory, Golden, CO, USA, with support from the U.S. DOE, Vehicle Technologies Office. NREL is operated by the Alliance for Sustainable Energy, LLC under Contract No. DE347AC36-99GO10337. M.A.R. thanks NREL colleagues Jon Luecke, Earl Christensen, Gina Chupka, and Lisa Fouts for their excellent technical contributions to this work. Finally, helpful input and guidance from Kenneth D. Rose, formerly of ExxonMobil, are gratefully acknowledged.

■ ABBREVIATIONS AND ACRONYMS

^{1}H = proton
^{13}C = carbon-13 (implies proton-decoupled ^{13}C NMR analysis)
1MN = 1-methylnaphthalene (see Figure 2)
2MHPD = 2-methylheptadecane (see Figure 2)
ADC = advanced distillation curve
AO = antioxidant (fuel additive)
ASTM = ASTM International (formerly American Society for Testing and Materials)
C = carbon
CF = grade no. 2-D S15 diesel emissions-certification fuel from Chevron-Phillips Chemical Co., batch A (aka CFA)
CI = compression ignition
C-K = chemical-kinetic
CN = cetane number
CP = cloud point
CRC = Coordinating Research Council, Inc.
CT = carbon type
D86 = ASTM D86 standard method and data
DCN = derived cetane number
DOE = Department of Energy
EBP = end boiling point
EOS = equation of state
FMP = final melting point
GC-FID = gas chromatography with flame ionization detection
GC×GC-FID = two-dimensional gas chromatography with flame ionization detection
GC×GC-SCD = two-dimensional gas chromatography with sulfur chemiluminescence detection
H = hydrogen
HMN = 2,2,4,4,6,8,8-heptamethylnonane (see Figure 2)
ID = ignition delay
IQT = ignition quality tester
LHV = lower heating value (aka net heat of combustion)
LI = lubricity improver (fuel additive)
MS = measured surrogate (a property value from a surrogate fuel)
MT = measured target (a property value from a target fuel)
NBCX = *n*-butylcyclohexane (see Figure 2)
NEI = *n*-eicosane (see Figure 2)
NHXD = n-hexadecane (see Figure 2)
NIST = National Institute of Standards and Technology
NMR = nuclear magnetic resonance spectroscopy
NOD = *n*-octadecane (see Figure 2)
PCER = palette-compound elution range
PHP = perhydrophenanthrene (see Figure 2)
PNNL = Pacific Northwest National Laboratory
ppmw = parts per million by weight
PS = predicted surrogate (a property predicted for a surrogate fuel)
SFC = supercritical fluid chromatography
SGT = silica-gel treatment
TDEC = *trans*-decalin (see Figure 2)
TET = tetralin (see Figure 2)
TIPB = 1,3,5-triisopropylbenzene (see Figure 2)
TIPCX = 1,3,5-triisopropylcyclohexane (see Figure 2)
TMB = 1,2,4-trimethylbenzene (see Figure 2)
ULSD = ultralow-sulfur diesel
U.S. = United States

■ REFERENCES

(1) Gieleciak, R.; Fairbridge, C. *Detailed Hydrocarbon Analysis of FACE Diesel Fuels Using Comprehensive Two-Dimensional Gas Chromatography*; CDEV-2013-2065-RT; CanmetENERGY: Devon, Alberta, Canada, 2013; http://www.crcao.org/publications/advancedVehiclesFuelsLubricants/FACE/GCxGC%20analysis%20of%20FACE%20fuels%20-RG%20v4%200%20Nov2013.pdf.

(2) Gieleciak, R.; Oro, N. *A Study of FID Response Factor of GC×GC Systems for Hydrocarbon Compound Classes Existing in Diesel Fractions*, CDEV-2013-1979-RT; CanmetENERGY: Devon, Alberta, Canada, 2013.

(3) Lemmon, E. W.; Huber, M. L.; McLinden, M. O. *NIST Reference fluid thermodynamic and transport properties database (REFPROP)*, NIST Standard Reference Database 23, Version 9.1; National Institute of Standards and Technology: Gaithersburg, MD, USA, 2013.

(4) Reiter, A. M.; Wallek, T.; Pfennig, A.; Zeymer, M. Surrogate Generation and Evaluation for Diesel Fuel. *Energy Fuels* **2015**, *29* (7), 4181−4192.

(5) Pitz, W. J.; Mueller, C. J. Recent progress in the development of diesel surrogate fuels. *Prog. Energy Combust. Sci.* **2011**, *37* (3), 330−350.

(6) Luo, J.; Yao, M.; Liu, H. A Reduced Chemical Kinetic Mechanism for Low Temperature Diesel Combustion and Soot Emissions. *Combust. Sci. Technol.* **2014**, *186* (12), 1975−1990.

(7) Wang, H.; Jiao, Q.; Yao, M. F.; Yang, B. B.; Qiu, L.; Reitz, R. D. Development of an n-heptane/toluene/polyaromatic hydrocarbon mechanism and its application for combustion and soot prediction. *Int. J. Engine Res.* **2013**, *14* (5), 434−451.

(8) Pei, Y.; Mehl, M.; Liu, W.; Lu, T.; Pitz, W. J.; Som, S. A Multicomponent Blend as a Diesel Fuel Surrogate for Compression Ignition Engine Applications. *J. Eng. Gas Turbines Power* **2015**, *137* (11), 111502.

(9) Pang, K. M.; Poon, H. M.; Ng, H. K.; Gan, S.; Schramm, J. *Soot Formation Modeling of n-Dodecane and Diesel Sprays under Engine-Like Conditions*, SAE Technical Paper 2015-24-2468; SAE International: Warrendale, PA, USA, 2015; DOI: 10.4271/2015-24-2468.

(10) Su, X.; Ra, Y.; Reitz, R. D. A Surrogate Fuel Formulation Approach for Real Transportation Fuels with Application to Multi-Dimensional Engine Simulations. *SAE Int. J. Fuels Lubr.* **2014**, *7* (1), 236−249.

(11) Ranzi, E.; Frassoldati, A.; Stagni, A.; Pelucchi, M.; Cuoci, A.; Faravelli, T. Reduced Kinetic Schemes of Complex Reaction Systems: Fossil and Biomass-Derived Transportation Fuels. *Int. J. Chem. Kinet.* **2014**, *46* (9), 512−542.

(12) Lin, R. H.; Tavlarides, L. L. Thermophysical properties needed for the development of the supercritical diesel combustion technology:

DOI: 10.1021/acs.energyfuels.5b02879
Energy Fuels 2016, 30, 1445−1461

Evaluation of diesel fuel surrogate models. *J. Supercrit. Fluids* **2012**, *71*, 136−146.
(13) Kwak, K. H.; Jung, D.; Borgnakke, C. Enhanced spray and evaporation model with multi-fuel mixtures for direct injection internal combustion engines. *Int. J. Engine Res.* **2014**, *15* (4), 488−503.
(14) Galle, J.; Verschaeren, R.; Verhelst, S. *The Behavior of a Simplified Spray Model for Different Diesel and Bio-Diesel Surrogates*, SAE Technical Paper 2015-01-0950; SAE International: Warrendale, PA, USA, 2015; DOI: 10.4271/2015-01-0950.
(15) Puduppakkam, K.; Naik, C.; Meeks, E.; Krenn, C.; Kroiss, R.; Gelbmann, J.; Pessl, G. *Predictive Combustion and Emissions Simulations for a High Performance Diesel Engine Using a Detailed Fuel Combustion Model*, SAE Technical Paper 2014-01-2570; SAE International: Warrendale, PA, USA, 2014; DOI: 10.4271/2014-01-2570.
(16) Naik, C. V.; Puduppakkam, K.; Meeks, E. Simulation and Analysis of In-Cylinder Soot Formation in a Low Temperature Combustion Diesel Engine Using a Detailed Reaction Mechanism. *SAE Int. J. Engines* **2013**, *6* (2), 1190−1201.
(17) Krishnasamy, A.; Reitz, R. D.; Willems, W.; Kurtz, E. *Surrogate Diesel Fuel Models for Low Temperature Combustion*, SAE Technical Paper 2013-01-1092; SAE International: Warrendale, PA, USA, 2013; DOI: 10.4271/2013-01-1092.
(18) McNenly, M. J.; Whitesides, R. A.; Flowers, D. L. Faster solvers for large kinetic mechanisms using adaptive preconditioners. *Proc. Combust. Inst.* **2015**, *35*, 581−587.
(19) Perini, F.; Krishnasamy, A.; Ra, Y.; Reitz, R. D. Computationally Efficient Simulation of Multicomponent Fuel Combustion Using a Sparse Analytical Jacobian Chemistry Solver and High-Dimensional Clustering. *J. Eng. Gas Turbines Power* **2014**, *136* (9), 091515.
(20) Dumitrescu, C. E.; Polonowski, C.; Fisher, B. T.; Cheng, A. S.; Lilik, G. K.; Mueller, C. J. An Experimental Study of Diesel-Fuel Property Effects on Mixing-Controlled Combustion in a Heavy-Duty Optical CI Engine. *SAE Int. J. Fuels Lubr.* **2014**, *7* (1), 65−81.
(21) Zhu, Y.; Davidson, D. F.; Hanson, R. K. Pyrolysis and oxidation of decalin at elevated pressures: A shock-tube study. *Combust. Flame* **2014**, *161* (2), 371−383.
(22) Haylett, D. R.; Davidson, D. F.; Hanson, R. K. Ignition delay times of low-vapor-pressure fuels measured using an aerosol shock tube. *Combust. Flame* **2012**, *159* (2), 552−561.
(23) Botero, M. L.; Mosbach, S.; Kraft, M. Sooting tendency of paraffin components of diesel and gasoline in diffusion flames. *Fuel* **2014**, *126*, 8−15.
(24) Bruno, T. J.; Fortin, T. J.; Lovestead, T. M.; Widegren, J. A. Chemical and Thermophysical Characterization of 1,3,5-Triisopropylcyclohexane. *J. Chem. Eng. Data* **2012**, *57* (8), 2343−2349.
(25) Mueller, C. J.; Cannella, W. J.; Bruno, T. J.; Bunting, B.; Dettman, H.; Franz, J.; Huber, M. L.; Natarajan, M.; Pitz, W. J.; Ratcliff, M. A.; Wright, K. Methodology for formulating diesel surrogate fuels with accurate compositional, ignition-quality, and volatility characteristics. *Energy Fuels* **2012**, *26* (6), 3284−3303.
(26) Hochhauser, A. M. *Review of prior studies of fuel effects on vehicle emissions*, E-84; Coordinating Research Council: Alpharetta, GA, USA, 2008; http://www.crcao.org/publications/emissions/index.html.
(27) Shapiro, F. R. *The Yale Book of Quotations*. Yale University Press: New Haven, CT, USA, 2006.
(28) Dryer, F. L. Chemical kinetic and combustion characteristics of transportation fuels. *Proc. Combust. Inst.* **2015**, *35* (1), 117−144.
(29) Lu, T.; Law, C. K. Toward accommodating realistic fuel chemistry in large-scale computations. *Prog. Energy Combust. Sci.* **2009**, *35* (2), 192−215.
(30) *Standard specification for diesel fuel oils*, ASTM Standard D975-15a; ASTM International: West Conshohocken, PA, USA, 2015; DOI:10.1520/D0975.
(31) Commercial equipment, instruments, or materials are identified only in order to adequately specify certain procedures. In no case does such identification imply recommendation or endorsement by the National Institute of Standards and Technology, nor does it imply that the products identified are necessarily the best available for the purpose.
(32) Farrell, J. T.; Cernansky, N. P.; Dryer, F. L.; Friend, D. G.; Hergart, C. A.; Law, C. K.; McDavid, R. M.; Mueller, C. J.; Patel, A. K.; Pitsch, H. *Development of an experimental database and kinetic models for surrogate diesel fuels*, SAE Technical Paper 2007-01-0201; SAE International: Warrendale, PA, USA, 2007; DOI: 10.4271/2007-01-0201.
(33) Wallace, L. A.; Renz, M. C. *Use of column chromatography to improve the ignition delay characteristics of impure methylcyclohexane in the ASTM D7170 FIT combustion analyzer*, Report to ASTM Subcommittee D02.01; Dixie Services: Galena Park, TX, USA, 2008.
(34) Japanwala, S.; Chung, K. H.; Dettman, H. D.; Gray, M. R. Quality of distillates from repeated recycle of residue. *Energy Fuels* **2002**, *16* (2), 477−484.
(35) *Standard test methods for instrumental determination of carbon, hydrogen, and nitrogen in petroleum products and lubricants*, ASTM Standard D5291-10; ASTM International: West Conshohocken, PA, USA, 2010: DOI: 10.1520/D5291.
(36) Rowley, R. L.; Wilding, W. V.; Knotts, T. A.; Giles, N. DIPPR Project 801: Evaluated Process Design Data, http://www.aiche.org/dippr/projects/801.
(37) Westbrook, C. K.; Pitz, W. J.; Mehl, M.; Curran, H. J. Detailed chemical kinetic reaction mechanisms for primary reference fuels for diesel cetane number and spark-ignition octane number. *Proc. Combust. Inst.* **2011**, *33*, 185−192.
(38) *Primary Reference Fuels (PRF) + PAH mechanism*, Version 1412; The CRECK Modeling Group, Milano, Italy, December 2014; http://creckmodeling.chem.polimi.it/index.php/menu-kinetics/menu-kinetics-detailed-mechanisms/menu-kinetics-prf-pah-mechanism. Accessed Oct. 27, 2015.
(39) Sarathy, S. M.; Westbrook, C. K.; Mehl, M.; Pitz, W. J.; Togbé, C.; Dagaut, P.; Wang, H.; Oehlschlaeger, M. A.; Niemann, U.; Seshadri, K.; Veloo, P. S.; Ji, C.; Egolfopoulos, F. N.; Lu, T. Comprehensive chemical kinetic modeling of the oxidation of 2-methylalkanes from C7 to C20. *Combust. Flame* **2011**, *158*, 2338−2357.
(40) Westbrook, C. K.; Pitz, W. J.; Herbinet, O.; Curran, H. J.; Silke, E. J. A comprehensive detailed chemical kinetic reaction mechanism for combustion of n-alkane hydrocarbons from n-octane to n-hexadecane. *Combust. Flame* **2009**, *156* (1), 181−199.
(41) LLNL Chemical Kinetic Mechanisms, Lawrence Livermore National Laboratory, Livermore, CA, USA; https://combustion.llnl.gov/. Accessed Oct. 27, 2015.
(42) Fournet, R.; Battin-Leclerc, F.; Glaude, P. A.; Judenherc, B.; Warth, V.; Côme, G. M.; Scacchi, G.; Ristori, A.; Pengloan, G.; Dagaut, P.; Cathonnet, M. The gas-phase oxidation of n-hexadecane. *Int. J. Chem. Kinet.* **2001**, *33* (10), 574−586.
(43) Yanowitz, J.; Ratcliff, M. A.; McCormick, R. L.; Taylor, J. D.; Murphy, M. J. *Compendium of experimental cetane numbers*, TP-5400-61693; National Renewable Energy Laboratory: Golden, CO, USA, 2014.
(44) Oehlschlaeger, M. A.; Steinberg, J.; Westbrook, C. K.; Pitz, W. J. The autoignition of iso-cetane at high to moderate temperatures and elevated pressures: Shock tube experiments and kinetic modeling. *Combust. Flame* **2009**, *156* (11), 2165−2172.
(45) Ranzi, E.; Frassoldati, A.; Faravelli, T.; Cuoci, A. Lumped Kinetic Modeling of the Oxidation of Isocetane (2,2,4,4,6,8,8-Heptamethylnonane) in a Jet-Stirred Reactor (JSR). *Energy Fuels* **2009**, *23*, 5287−5289.
(46) Weber, B. W.; Pitz, W. J.; Mehl, M.; Silke, E. J.; Davis, A. C.; Sung, C. J. Experiments and modeling of the autoignition of methylcyclohexane at high pressure. *Combust. Flame* **2014**, *161* (8), 1972−1983.
(47) Mechanism of Real Transportation Fuels (Gasoline, Jet Fuels, Diesel: PRFs, heavy n-alkanes, Isocetane, Decalin, Tetralin, etc.); Version 1412, December 2014, The CRECK Modeling Group, http://creckmodeling.chem.polimi.it/index.php/menu-kinetics/menu-kinetics-detailed-mechanisms/menu-kinetics-prf-pah-real-fuels-mechanism. Accessed Oct. 27, 2015.

DOI: 10.1021/acs.energyfuels.5b02879
Energy Fuels 2016, 30, 1445−1461

(48) Honnet, S.; Seshadri, K.; Niemann, U.; Peters, N. A surrogate fuel for kerosene. *Proc. Combust. Inst.* **2009**, *32* (1), 485−492.
(49) Bounaceur, R.; Glaude, P. A.; Fournet, R.; Battin-Leclerc, F.; Jay, S.; Pires Da Cruz, A. Kinetic modelling of a surrogate diesel fuel applied to 3D auto-ignition in HCCI engines. *Int. J. Veh. Des.* **2007**, *44* (1/2), 124−142.
(50) Wang, H.; Warner, S. J.; Oehlschlaeger, M. A.; Bounaceur, R.; Biet, J.; Glaude, P. A.; Battin-Leclerc, F. An experimental and kinetic modeling study of the autoignition of alpha-methylnaphthalene/air and alpha-methylnaphthalene/n-decane/air mixtures at elevated pressures. *Combust. Flame* **2010**, *157* (10), 1976−1988.
(51) Linstrom, P. J., Mallard, W. G. *NIST Chemistry WebBook*, NIST Standard Reference Database No. 69; National Institute of Standards and Technology, Gaithersburg, MD, USA, http://webbook.nist.gov. Accessed Oct. 27, 2015.
(52) Gough, R. V.; Widegren, J. A.; Bruno, T. J. Thermal Decomposition Kinetics of 1,3,5-Triisopropylcyclohexane. *Ind. Eng. Chem. Res.* **2013**, *52* (24), 8200−8205.
(53) Gieleciak, R. M. *Analysis and purity estimation of products of hydrogenation of phenanthrene*, presentation to CRC Project AVFL-18a Panel, Sep. 26, 2013.
(54) Heyne, J. S.; Boehman, A. L.; Kirby, S. Autoignition studies of trans- and cis-decalin in an ignition quality tester (IQT) and the development of a high thermal stability unifuel/single battlefield fuel. *Energy Fuels* **2009**, *23*, 5879−5885.
(55) *Standard test method for determination of ignition delay and derived cetane number (DCN) of diesel fuel oils by combustion in a constant volume chamber*, ASTM Standard D6890-13b; ASTM International: West Conshohocken, PA, USA, 2013; DOI: 10.1520/D6890.
(56) Bruno, T. J.; Ott, L. S.; Smith, B. L.; Lovestead, T. M. Complex fluid analysis with the advanced distillation curve approach. *Anal. Chem.* **2010**, *82*, 777−783.
(57) Bruno, T. J.; Ott, L. S.; Lovestead, T. M.; Huber, M. L. The composition explicit distillation curve technique: relating chemical analysis and physical properties of complex fluids. *J. Chromatogr. A* **2010**, *1217* (16), 2703−2715.
(58) Bruno, T. J.; Ott, L. S.; Lovestead, T. M.; Huber, M. L. Relating complex fluid composition and thermophysical properties with the advanced distillation curve approach. *Chem. Eng. Technol.* **2010**, *33* (3), 363−376.
(59) *Standard test method for density, relative density, and API gravity of liquids by digital density meter*, ASTM Standard D4052-11; ASTM International: West Conshohocken, PA, USA, 2011; DOI: 10.1520/D4052.
(60) Mendenhall, G. D. Eastern Sources, Spring Valley, NY, USA; http://www.easternsourcess.com/. Accessed Oct. 14, 2015.
(61) Fisher Scientific. https://www.fishersci.com/us/en/home.html. Accessed Oct. 14, 2015.
(62) Sigma Aldrich. http://www.sigmaaldrich.com/united-states.html. Accessed Oct. 14, 2015.
(63) TCI America. http://www.tcichemicals.com/en/us/. Accessed Oct. 14, 2015.
(64) Gieleciak, R. M. *The purity of [palette] compounds based on GC×GC-FID analysis*, presentation to CRC Project AVFL-18a Panel, Sep. 20, 2014.
(65) Gieleciak, R. M. *2-Methylheptadecane*, presentation to CRC Project AVFL-18a Panel, Oct. 22, 2014.
(66) *Chemical Hazards and Toxic Substances*, U.S. Department of Labor, Occupational Safety & Health Administration (OSHA), Washington, DC, USA; https://www.osha.gov/SLTC/hazardoustoxicsubstances/. Accessed Oct. 26, 2015.
(67) Jackson, H. L.; McCormack, W. B.; Rondestvedt, C. S.; Smeltz, K. C.; Viele, I. E. Control of peroxidizable compounds. *J. Chem. Educ.* **1970**, *47* (3), A175.
(68) Türker, L.; Variş, S. JP-900 Hydroperoxidation and Decomposition. *Propellants, Explos., Pyrotech.* **2014**, *39* (2), 211−216.
(69) *Safety Data Sheet for 1-Methylnaphthalene*, Version 5.11; Sigma-Aldrich: St. Louis, MO, USA, 2014.
(70) Gieleciak, R.; Hager, D. *Estimation of purity of compounds for diesel fuel surrogate blends*, Division Report Devon 10-68 (CF); CanmetENERGY; Devon, Alberta, Canada, 2010.
(71) *Standard test method for determination of total sulfur in light hydrocarbons, spark ignition engine fuel, diesel engine fuel, and engine oil by ultraviolet fluorescence*, ASTM Standard D5453-12; ASTM International: West Conshohocken, PA, USA, 2012; DOI: 10.1520/D5453.
(72) Matzke, M.; Litzow, U.; Jess, A.; Caprotti, R.; Balfour, G. Diesel Lubricity Requirements of Future Fuel Injection Equipment. *SAE Int. J. Fuels Lubr.* **2009**, *2* (1), 273−286.
(73) Ghosh, P.; Jaffe, S. B. Detailed composition-based model for predicting the cetane number of diesel fuels. *Ind. Eng. Chem. Res.* **2006**, *45* (1), 346−351.
(74) *Standard test method for boiling range distribution of petroleum fractions by gas chromatography*, ASTM Standard D2887-14; ASTM International: West Conshohocken, PA, USA, 2014; DOI: 10.1520/D2887.
(75) *Standard test method for distillation of petroleum products at atmospheric pressure*, ASTM Standard D86-12. ASTM International: West Conshohocken, PA, USA, 2012; DOI: 10.1520/D0086.
(76) Burger, J. L.; Harries, M. E.; Bruno, T. J. *Characterization of Four Diesel Fuel Surrogates by the Advanced Distillation Curve Method* **2015**, manuscript in preparation.
(77) Dumitrescu, C. E.; Polonowski, C. J.; Fisher, B. T.; Lilik, G. K.; Mueller, C. J. Diesel Fuel Property Effects on In-Cylinder Liquid Penetration Length: Impact on Smoke Emissions and Equivalence Ratio Estimates at the Flame Lift-Off Length. *Energy Fuels* **2015**, *29*, 7689.
(78) Fisher, B. T.; Knothe, G.; Mueller, C. J. Liquid-phase penetration under unsteady in-cylinder conditions: Soy- and cuphea-derived biodiesel fuels versus conventional diesel. *Energy Fuels* **2010**, *24* (9), 5163−5180.
(79) *Standard test method for heat of combustion of liquid hydrocarbon fuels by bomb calorimeter (precision method)*, ASTM Standard D4809-09a; ASTM International: West Conshohocken, PA, USA, 2009; DOI: 10.1520/D4809.
(80) *Standard Test Method for Evaluating Lubricity of Diesel Fuels by the High-Frequency Reciprocating Rig (HFRR)*, ASTM Standard D6079-11; ASTM International: West Conshohocken, PA, USA, 2011; DOI: 10.1520/D6079.
(81) *Standard test method for cloud point of petroleum products (constant cooling rate method)*, ASTM Standard D5773-15; ASTM International: West Conshohocken, PA, USA, 2015; DOI: 10.1520/D5773.
(82) Chupka, G. M.; Fouts, L.; McCormick, R. L. Effect of low-level impurities on low-temperature performance properties of biodiesel. *Energy Environ. Sci.* **2012**, *5* (9), 8734−8742.
(83) *Standard test method for smoke point of kerosine and aviation turbine fuel*, ASTM Standard D1322-15; ASTM International: West Conshohocken, PA, USA, 2015; DOI: 10.1520/D1322.
(84) *Standard test method for determination of the aromatic content and polynuclear aromatic content of diesel fuels and aviation turbine fuels by supercritical fluid chromatography*, ASTM Standard D5186-15; ASTM International: West Conshohocken, PA, USA, 2015: DOI: 10.1520/D5186.
(85) *Standard Test Methods for Flash Point by Pensky-Martens Closed Cup Tester*, ASTM Standard D93-11; ASTM International: West Conshohocken, PA, USA, 2011; DOI: 10.1520/D0093.
(86) *Standard Test Method for Corrosiveness to Copper from Petroleum Products by Copper Strip Test*, ASTM Standard D130-10; ASTM International: West Conshohocken, PA, USA, 2010; DOI: 10.1520/D0130.
(87) *Standard Test Method for Kinematic Viscosity of Transparent and Opaque Liquids (and Calculation of Dynamic Viscosity)*, ASTM Standard D445-11a; ASTM International: West Conshohocken, PA, USA, 2011; DOI: 10.1520/D0445.

DOI: 10.1021/acs.energyfuels.5b02879
Energy Fuels 2016, 30, 1445−1461